AD-A047 262 ARIZONA UNIV TUCSON ENGINEERING EXPERIMENT STATION F/G 20/13
CONVECTION IN THE CLOSED BRAYTON CYCLE.(U)
APR 77 P E PICKET, D M MCELIGOT, M F TAYLOR N00014-75-C-0694
UNCLASSIFIED 1248-5 NL

OF
AD
A047262

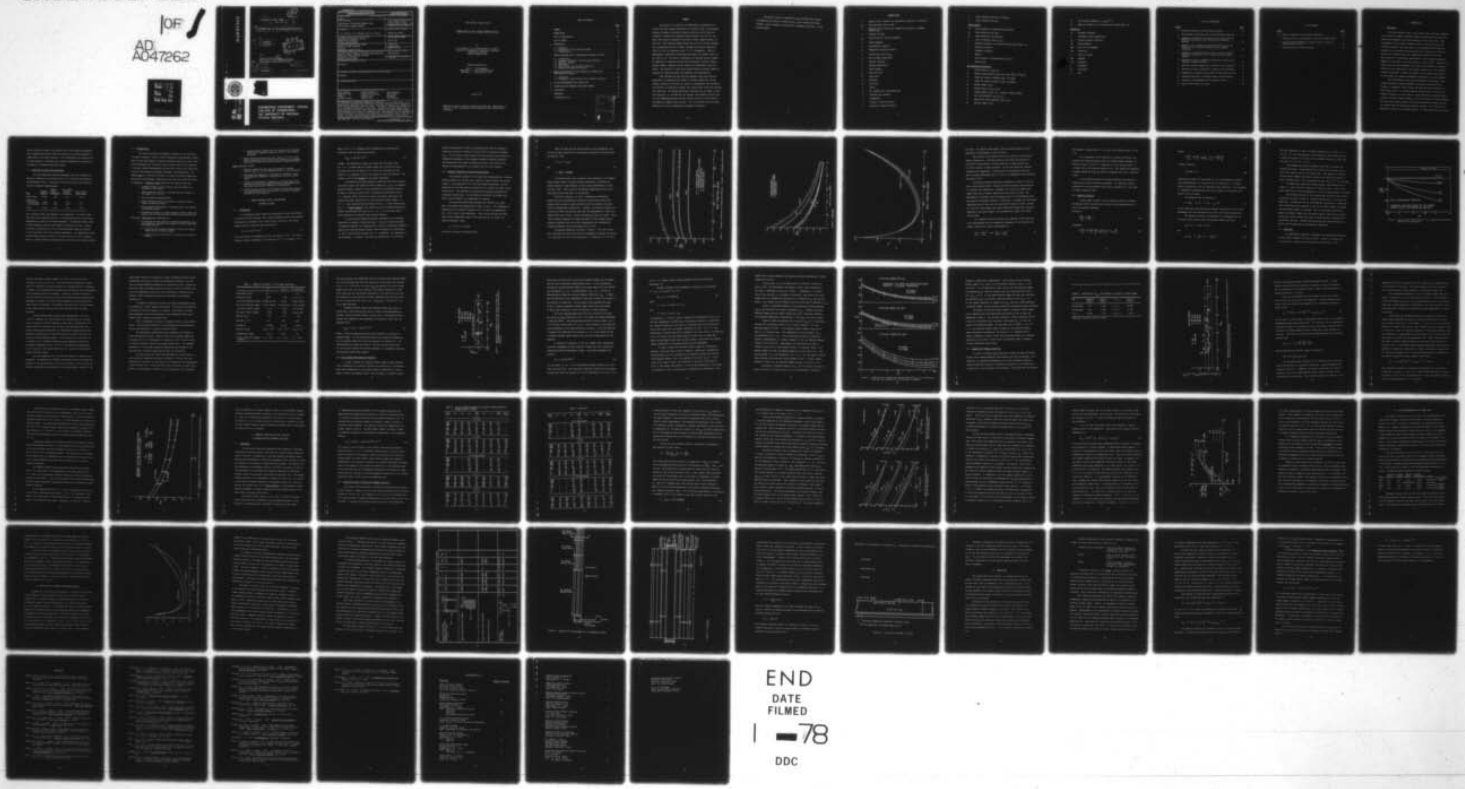

END
DATE
FILMED
1 -78
DDC

(11) BS.

(9) Third Annual Summary Report, no. 3
1 Apr 76-31 Mar 77,

(6) CONVECTION IN THE CLOSED BRAYTON CYCLE.

by

(10) P. E. Picket,
D. M. McEligot
M. F. Taylor

for

(15) Office of Naval Research
ONR Contract Number N00014-75-C-0694
ONR Contract Authority NR-097-395

(14) 1248-5

(12) 71 p.

(11) 1 April 1977

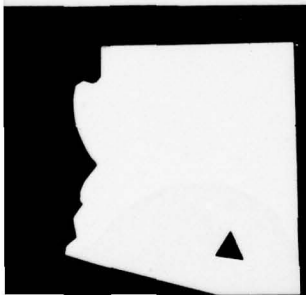

Unclassified

SECURITY CLASSIFICATION OF THIS PAGE (When Data Entered)

REPORT DOCUMENTATION PAGE		READ INSTRUCTIONS BEFORE COMPLETING FORM
1. REPORT NUMBER 1248-5	2. GOVT ACCESSION NO.	3. RECIPIENT'S CATALOG NUMBER
4. TITLE (and Subtitle) CONVECTION IN THE CLOSED BRAYTON CYCLE (Third Annual Summary Report)		5. TYPE OF REPORT & PERIOD COVERED Annual Summary Report 1 April 1976 - 31 Mar. 1977 6. PERFORMING ORG. REPORT NUMBER
7. AUTHOR(s) P. E. Pickett, D. M. McEligot and M. F. Taylor		8. CONTRACT OR GRANT NUMBER(s) N00014-75-C-0694
9. PERFORMING ORGANIZATION NAME AND ADDRESS Engineering Experiment Station University of Arizona Tucson, Arizona 85721		10. PROGRAM ELEMENT, PROJECT, TASK AREA & WORK UNIT NUMBERS NR 097-395
11. CONTROLLING OFFICE NAME AND ADDRESS Office of Naval Research Code 473 Arlington, Virginia 22217		12. REPORT DATE 1 April 1977 13. NUMBER OF PAGES 73
14. MONITORING AGENCY NAME & ADDRESS(if different from Controlling Office) Office of Naval Research, Resident Representative Room 421, Space Sciences Building University of Arizona Tucson, Arizona 85721		15. SECURITY CLASS. (of this report) Unclassified 15a. DECLASSIFICATION/DOWNGRADING SCHEDULE

16. DISTRIBUTION STATEMENT (of this Report)

Unlimited

17. DISTRIBUTION STATEMENT (of the abstract entered in Block 20, if different from Report)

Unlimited

18. SUPPLEMENTARY NOTES

19. KEY WORDS (Continue on reverse side if necessary and identify by block number)

Heat Transfer	Forced Convection	Heat Exchangers
Turbulent Flow	Turbulence Structure	Noble Gases
Tubes	Brayton Cycle	Roughness
Boundary Layers	Laminar Flow	Gas Mixtures

20. ABSTRACT (Continue on reverse side if necessary and identify by block number)

To correspond to conditions expected in components in the closed Brayton cycle, analyses and experiments were conducted for forced convective heat transfer to gases and gas mixtures flowing in ducts. The range of interest was $0.2 \lesssim Pr \lesssim 0.7$, representing mixtures of inert gases. Numerical analyses predicted that existing scaling laws for gases would not represent the Prandtl number dependence adequately for laminar or turbulent flow. Measurements with an argon-helium mixture confirmed the trends of the predictions for turbulent flow in circular tubes. The wall turbulent Prandtl number was determined for $0.4 \lesssim Pr \lesssim 0.5$.

DD FORM 1 JAN 73 1473 EDITION OF 1 NOV 65 IS OBSOLETE

$\lesssim$ = or < than

Unclassifed

SECURITY CLASSIFICATION OF THIS PAGE (When Data Entered)

Third Annual Summary Report

CONVECTION IN THE CLOSED BRAYTON CYCLE

By

P. E. Pickett, D. M. McEligot and M. F. Taylor
Aerospace and Mechanical Engineering Department
University of Arizona
Tucson, Arizona 85721

Research Sponsored by

Office of Naval Research
ONR Contract Number N00014-75-C-0694
ONR Contract Authority NR-097-395

1 April 1977

TABLE OF CONTENTS

SUMMARY

The results of a numerical and experimental investigation of friction and heat transfer parameters for turbulent flow of helium-argon mixtures in smooth, electrically heated, vertical circular tubes are presented. Mixtures with molecular weights between 15.3 and 29.7 are used; these values correspond to molecular Prandtl numbers between 0.42 and 0.49. Inlet Reynolds numbers range from 31,200 to 102,000, maximum wall temperatures from 392 to 828°K, maximum wall-to-bulk temperature ratios to 1.82, and pressures from 4.7 to 9.7 atmospheres. Existing experimental correlations, developed using gases with Prandtl numbers of the order of 0.7, are found to overpredict the observed Nusselt numbers. By comparison of numerical calculations and measured constant property Nusselt numbers, turbulent Prandtl numbers are determined in the wall region. The validity of using these deduced turbulent Prandtl numbers is examined for conditions where the properties vary significantly.

Heat transfer and wall friction parameters have been obtained numerically to demonstrate the effects of mixture composition and gas property variation for heating or cooling in regenerative heat exchangers. The situation is modelled by laminar flow through short ducts with constant wall heat flux. For design predictions accounting for the effect of property variation, it is found that the property ratio method is better than the film temperature method for heat transfer while the latter method is preferable for apparent wall friction - with the proviso that the present definitions of the non-dimensional parameters be employed.

The present status of experiments using alternate gas mixtures and examining the effects of heating rate on heat transfer from rough surfaces, such as ceramics or artificially roughened superalloys, is presented briefly.

NOMENCLATURE

a	exponent used to account for temperature variation of viscosity;
A_{cs}	cross sectional area of tube;
b	exponent used to account for temperature variation of thermal conductivity;
c	velocity of sound;
c_p	specific heat at constant pressure;
D	inside diameter;
g	gravitational constant;
g_c	dimensional conversion factor;
G	average mass flux, $\dot{m}/A_{cs}$;
h	heat transfer coefficient;
i	specific enthalpy;
k	thermal conductivity;
ℓ	mixing length;
$\dot{m}$	mass flow rate;
$\tilde{M}$	molal mass;
p	pressure;
q''	heat flux;
r	radius;
R	gas constant for a particular gas;
$\bar{R}$	universal gas constant;
T	temperature;
u	velocity in axial direction;
v	velocity in radial direction;

x axial distance from start of heating;

y radial distance from wall.

Greek Symbols

ε/κ force constant in Lennard-Jones potential;

ε_H eddy diffusivity for heat;

ε_M eddy diffusivity for momentum;

γ ratio of specific heats, c_p/c_v;

κ empirical constant in van Driest mixing length model, 0.4;

μ absolute viscosity;

ν kinematic viscosity;

ρ density;

σ force constant in Lennard-Jones potential;

τ shear stress.

Non-dimensional Parameters

f friction factor, $2g_c\rho\tau_w/G^2$;

Gr Grashof number based on wall heat flux, $gD^4q"_w/(\nu^2\mu c_p T)_i$;

L^+ length for velocity boundary layer, $4L/(D_h Re)$

L^* length for thermal boundary layer, $4L/(D_h RePr)$

Nu Nusselt number, hD/k;

$\bar{p}$ pressure drop, $\rho_i g_c(p_i-p)/G^2$;

Pr Prandtl number, $c_p\mu/k$; Pr_t, turbulent Prandtl number;

q^+ heat flux parameter, $q"_w/(Gc_{p,i}T_i)$;

Q^+ laminar heat flux parameter, $q"_w D_h/(k_i T_i)$;

Re Reynolds number, GD/μ;

y^+ wall distance parameter, $y(g_c\tau_w/\rho)^{1/2}/\nu$;

y_ℓ^+ empirical constant in van Driest mixing length model, 26.

Subscripts

av lengthwise average;

b evaluated at bulk temperature;

cp constant property condition;

DB Dittus-Boelter;

DKM Drew, Koo and McAdams;

eff effective;

i inlet; an index;

Max maximum;

ref reference;

t turbulent;

VD van Driest;

w wall.

LIST OF ILLUSTRATIONS

LIST OF TABLES

I. INTRODUCTION

1.1. Background

The closed Brayton cycle, or gas turbine cycle, has been suggested as an efficient, compact, versatile system for power plant and propulsion applications [Bammert, Rurik and Griepentrog, 1974; Mock, 1970]. With thermodynamic cycle studies, Bammert and Klein [1974] showed that considerable savings in the total costs of the turbomachines and heat exchangers can be achieved by mixing helium with a heavier gas. When the heavier gas is another noble gas, approximate calculations indicate the possibility of significant improvements in heat transfer performance compared to pure gases at the same conditions [Vanco, 1965]. However, the gaseous data for heat exchangers and analyses for idealized, but related, conditions have concentrated on pure gases, primarily air, with constant transport properties. Whether such results can be applied for mixtures of inert gases with temperature-dependent properties is a basic question.

The closed Brayton cycle offers advantages of reliability, high thermal efficiency, reduced atmospheric pollution, minimal erosion or blockage of components, rapid startup and high part-load efficiency to a wide range of uses. It has been proposed for application to surface and undersea propulsion of naval ships in conjunction with gas-cooled nuclear reactors and fossil fueled combustors, and for auxiliary electrical systems, for solar power, power systems for satellites and space stations, bus and rail power plants and refrigeration/heating systems. Cycle efficiency is expected to improve as technology advances. By employing noble gas mixtures

such as helium and xenon as the working fluid, heat transfer performance can be improved and system volume and weight can be reduced compared to common gases at the same conditions. The understanding and effective use of these methods of increasing heat transfer performance are important to the design of lightweight propulsion plants.

1.2. Conditions In Naval Brayton Systems

The non-dimensional governing parameters have been estimated for operating conditions in the Brayton test unit at the Naval Ship Research and Development Center. With argon as the working fluid, the following values are expected (approximately).

Unit	Reynolds Number	Grashof Number (buoyancy)	Mach Number (Compress-ibility)	Wall-to-Bulk Temp. Ratio
Heater Tubes	50,000	560	0.3	1.15
Recuperator				
Low Pressure	1,800	110	0.06	0.9
High Pressure	2,700	160	0.05	1.1
Cooler	2,300	2,000	0.04	0.85

Thus, buoyancy effects are expected to be unimportant. The heater tubes would have fully turbulent flow and, in further modification of the design, compressibility effects could become important. The Reynolds number range in heat exchangers implies either laminar or transitional flow. Laminar flow might be predicted well with a three-dimensional numerical analysis but the transition region would require experiments. The temperature ratios indicate modest property variation in present designs but with a graphite heater or ceramic components extreme property variation could become involved.

1.3. Proposed Work

The initial proposal and subsequent proposals by the University of Arizona [McEligot, 1974a,b, 1975a,b] detailed the applications, advantages of inert gas mixtures, convective problems, prediction of heat transfer and pressure drop, scientific needs, previous work at the University of Arizona, proposed experimental and analytical studies and related work, facilities and apparatus available, personnel, and nomenclature. The general goal is to develop the ability to predict accurately temperature and velocity distributions, pressure drop and wall heat fluxes for flows in components. Scientific needs related to the proposed work were:

1. Determine whether existing scaling laws are adequate for mixtures of inert gases.
2. Extend numerical analyses to include inert gas mixtures in the range $0.2 \lesssim Pr \lesssim 0.7$.
3. Test the analyses experimentally.
4. Obtain definitive data on the effect of molecular Prandtl number on turbulence models.
5. Obtain greater understanding of turbulent shear flow through the proposed studies.
6. Determine the effects of element geometry, Prandtl number and heating rate on convective heat transfer from rough surfaces.

Accordingly, objectives were summarized as:

1. For mixtures of inert gases with temperature-dependent transport properties, determine the effects of mixture composition and heating rate on:
   a. convective heat transfer parameters, such as the Nusselt number and/or the Stanton number,
   b. pressure drop or wall friction, in terms of the friction factor,

c. convective heat transfer and fluid friction for flow over artificially roughened surfaces in terms of the roughness functions.

2. Extend theoretical predictions into range $0.2 \lesssim Pr \lesssim 0.7$ and improve understanding of turbulent heat transfer with property variations for both smooth and artificially roughened surfaces.

Tasks suggested include:

1. Numerical predictions for inert gas mixtures in heated circular tubes as in some proposed heaters for ship propulsion.

2. Preliminary measurements of pure gases and mixtures in open-loop apparatus; comparison to predictions (first and second years).

3. Design and modifications of apparatus to provide closed loop operation with the more expensive mixtures; measurements with pure gases and mixtures; comparison to predictions.

4. Design and fabrication of test sections to obtain mean velocity and temperature profiles for flow over artificially roughened surfaces with heat addition.

2. HEATED TURBULENT FLOW OF HELIUM-ARGON MIXTURES IN TUBES

2.1. Introduction

In preliminary design studies for application of inert gas mixtures to closed gas turbine systems, Vanco [1965] estimated relative heat transfer coefficients for turbulent flow in ducts using a version of the Colburn analogy [Kreith, 1958] which may be written as:

$$Nu = 0.023\ Re^{0.8}\ Pr^{1/3} \tag{1}$$

This relationship is supposedly valid for the range $0.5 < Pr < 100$, but is primarily based on experiments for fluids with $Pr \gtrsim 0.7$ or greater. For

gases, with Pr $\tilde{\sim}$ 0.7, McAdams [1954] recommended the Dittus-Boelter correlation with the coefficient modified

$$Nu_{DB} = 0.021\ Re^{0.8}\ Pr^{0.4} \tag{2}$$

instead. The difference is about ten percent for most gases (with Pr $\tilde{\sim}$ 0.7). As shown later the Prandtl number for a mixture of helium and argon can be of the order of 0.4; no data are available for this range so it is important to test the validity of these correlations. This testing is one of the purposes of the present experiment.

For predictions of heat transfer to turbulent flows many engineering analyses employ the turbulent Prandtl number, $Pr_t = \varepsilon_m/\varepsilon_h$, to estimate effective thermal conductivity from correlations for momentum transfer. As shown in surveys by Blom [1970], by Quarmby and Quirk [1972] and by A. J. Reynolds [1975], there still exists considerable uncertainty concerning the proper variation of Pr_t with molecular Prandtl number. At Pr $\tilde{\sim}$ 0.7, some idealized analyses suggest that $Pr_t > 1$ while others yield $Pr_t < 1$. A second purpose of the present work is to determine whether Pr_t differs significantly from unity at Pr $\tilde{\sim}$ 0.4 - 0.5 in the wall region, which dominates the convective heat transfer behavior.

The next section summarizes pertinent knowledge of the transport properties of mixtures of helium and argon. Section 3 briefly describes the numerical analysis to be employed and, for fully established conditions, presents the predicted Nusselt numbers, which disagree with correlations (1) and (2) when Reynolds analogy ($Pr_t = 1$) is employed. The experiment is then described. In Section 5 the data are extrapolated to the constant

property idealization to test the correlations and then the diagnostic technique of McEligot, Pickett and Taylor [1976] is applied to estimate $Pr_{t,w}$. The following section extends the data to heating rates where the temperature dependence of the transport properties becomes significant and demonstrates that numerical predictions based on the value of Pr_t deduced from measurements at low heating rates are still adequate.

2.2. Transport Properties of Helium-Argon Mixtures

The properties needed for this study were compressibility, viscosity, thermal conductivity, specific heat, enthalpy, speed of sound, and the gas constant. The properties of air have been studied extensively; for the comparison data the NBS tables of Hilsenrath et al.[1955] were used in this investigation. The properties of helium and helium-argon mixtures were calculated theoretically. For all gases the viscosity and thermal conductivity were assumed to be independent of pressure.

The helium and helium-argon mixtures were assumed to be ideal gases, thus making the compressibility equal to unity. This assumption is reasonable for the range of pressures (100 - 970 kPa) and temperatures (290 - 830°K) used in this experiment. Since helium and argon are monatomic and the temperature range in this study was not too large, the relation [Reynolds, 1968]

$$c_p = (5/2)\ R = (5/2)R/\tilde{M} \tag{3}$$

was used to calculate the specific heat.

Using the ideal gas and constant specific heat assumptions, one may derive simple equations for the enthalpy and speed of sound [Reynolds and Perkins, 1968]

$$i = c_p (T - T_{ref})$$

and (4)

$$c = \sqrt{\gamma RT} = \sqrt{(5/3)RT}$$

The Lennard-Jones (6-12) potential can be employed in the Chapman-Enskog kinetic theory to predict thermal conductivity, viscosity and Prandtl number of binary mixtures of inert gases [Hirschfelder, Curtiss and Bird, 1964]. There has been considerable experimental study of the pure gases but few data exist on the mixtures.

With force constants, ε/κ and σ, suggested by Hirschfelder, Curtiss and Bird the predicted viscosity for helium falls about eight percent below the data of Dawe and Smith [1970] and Kalelkar and Kestin [1970] at temperatures around 900°C. Likewise, the predicted thermal conductivity is about nine percent lower than the measurements of Saxena and Saxena [1968] up to 1100°C. Similar discrepancies exist for argon. Using force constants suggested by DiPippo and Kestin [1969] instead leads to essential agreement with the values recommended by the Thermophysical *Properties Research Center* [Touloukian and Ho, 1970].

The mixture properties are shown in Figure 1. The solid curves were calculated with the force constants recommended by DiPippo and Kestin: σ = 2.158A and ε/κ = 86.2 K for helium and σ = 3.292A and $\varepsilon/\kappa \approx$ 152.75°K

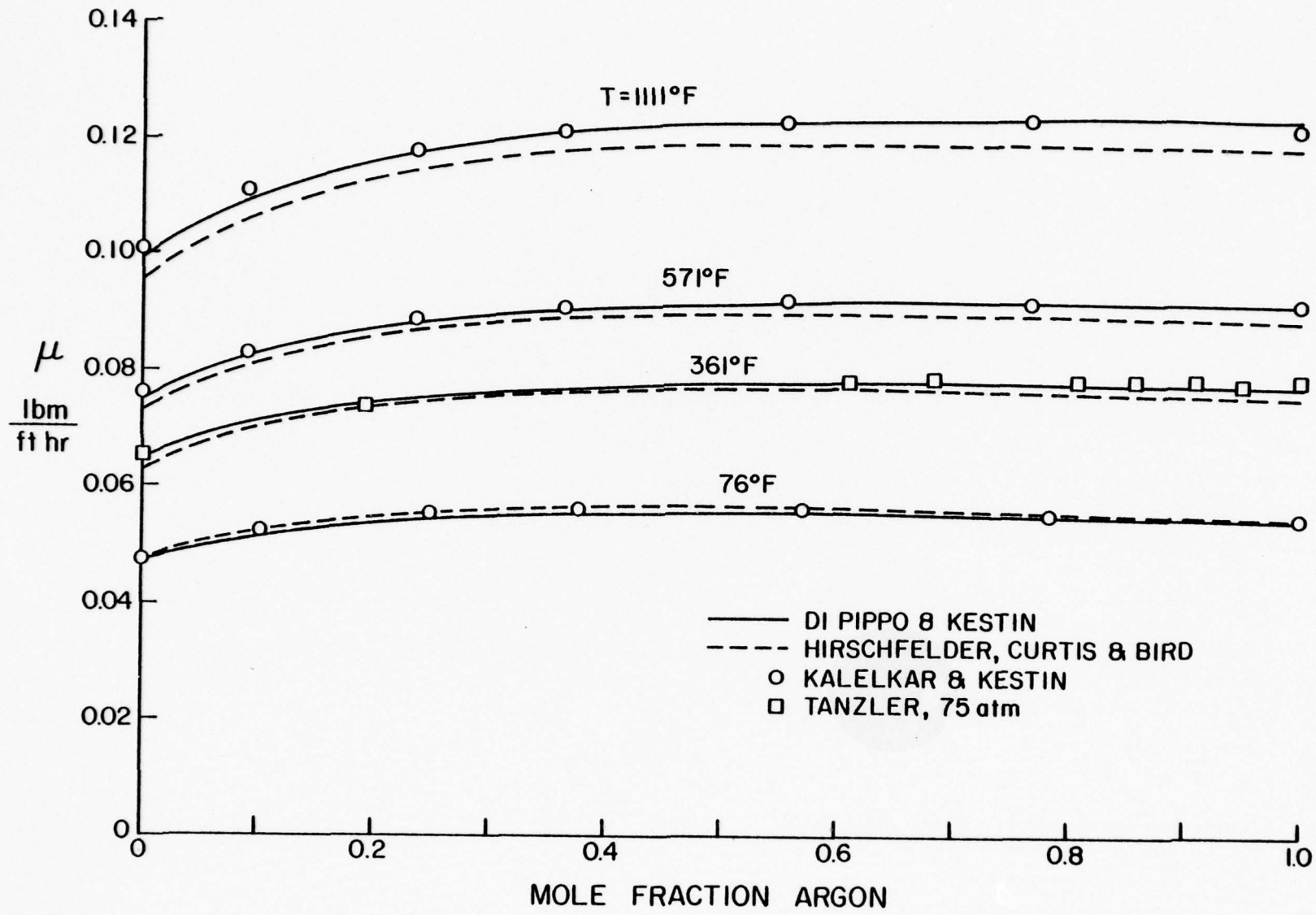

Figure 1. Transport Properties of Helium-argon Mixtures. Pressure = 1 Atmosphere unless noted.

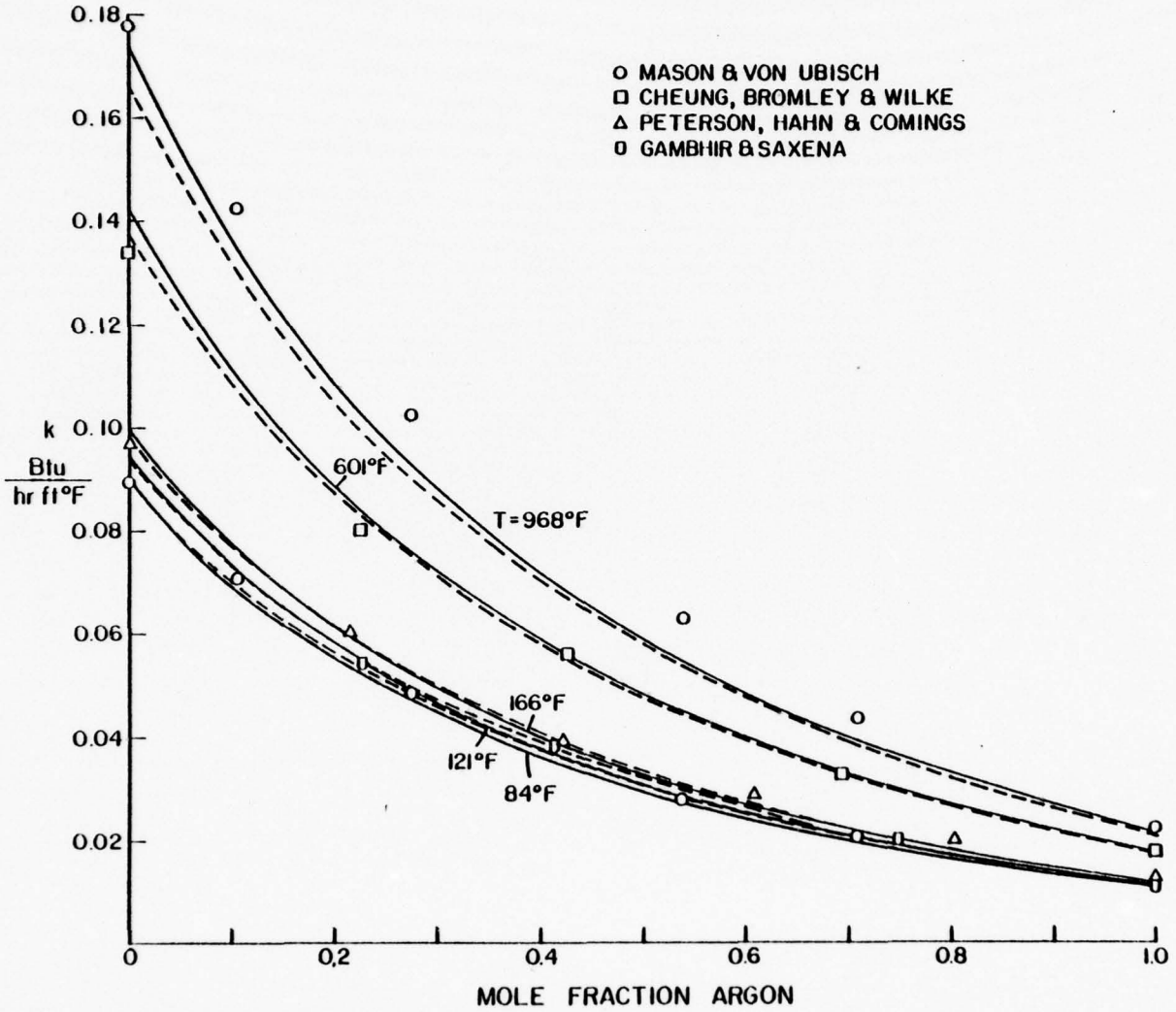

Figure 1.--Continued

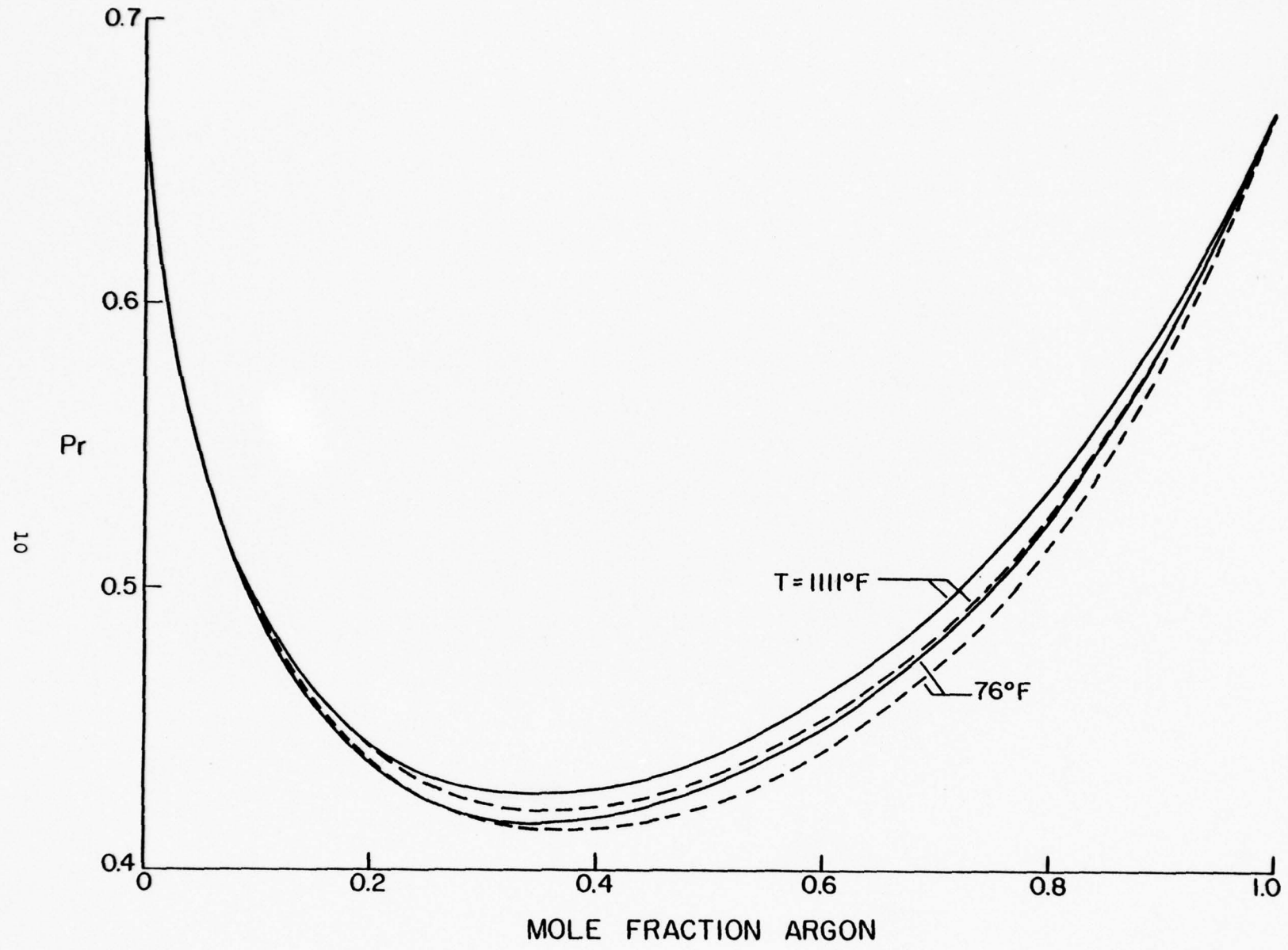

Figure 1.--Continued

for argon. The dashed curves compare values calculated from the recommendations of Hirschfelder, Curtiss and Bird.

The viscosity of the mixture varies only slightly with molecular weight (composition). From pure helium to pure argon the variation is only about fifteen percent; for mole fractions of argon greater than 0.25 the viscosity is almost constant. As with pure gases the viscosity increases with temperature. The predicted values agree well with the data of Tanzler [Touloukian and Ho, 1970] at 75 atmospheres and of Kalelkar and Kestin [1970].

The mixture thermal conductivity decreases by a factor of five or more as the molecular weight increases from pure helium to pure argon and it increases with temperature. Agreement with the data of Gambhir and Saxena [1966] and of Cheung, Bromley and Wilke [1962] is close. The measurements of Peterson, Hahn and Commings [1971] at 50 atmospheres show that neglect of pressure variation is justified. It appears that the higher temperature data of Mason and von Ubisch [1960] refute the model; however, in a critical review Gandhi and Saxena [1958] have observed that the measurements of von Ubisch appear to be systematically higher than others they reviewed.

In a companion study for laminar flow, McEligot, Taylor and Durst [1977] demonstrated that the temperature dependence of the viscosity and thermal conductivity could be approximated as

$$\frac{\mu}{\mu_{ref}} = \left(\frac{T}{T_{ref}}\right)^{a} \quad \text{and} \quad \frac{k}{k_{ref}} = \left(\frac{T}{T_{ref}}\right)^{b} \tag{5}$$

The exponent a ranges from 0.7 to 0.8 and b falls between about 0.7 and 0.75.

As a consequence of the variation of thermal conductivity and specific heat versus molecular weight the Prandtl number decreases to a minimum of about 0.42 at $\tilde{M} \tilde{\sim} 16$ from about 2/3 for the pure gases. It is about 0.48 at the molecular weight of air. The temperature dependence is almost negligible since the power law exponents for μ and k differ so little.

In the present study the calculated properties were applied in tabular form in the data reduction programs. For numerical analyses, correlations of the calculated values--such as equations (5)--were used to reduce computation time.

2.3. Numerical Analysis

In this paper, analysis is by the numerical method of Bankston and McEligot [1970] utilizing finite control volume approximations to solve the governing equations,

Continuity:

$$\frac{\partial\ \hat{\rho}\hat{u}}{\partial\bar{x}} + \frac{1}{\bar{r}}\frac{\partial \bar{r}\hat{\rho}\hat{v}}{\partial\bar{r}} = 0 \tag{6a}$$

x-momentum:

$$\hat{\rho}\hat{u}\frac{\partial\hat{u}}{\partial\bar{x}} + 2\hat{\rho}\hat{v}\frac{\partial\bar{u}}{\partial\bar{r}} = \frac{d\bar{p}}{d\bar{x}} + \frac{4}{Re_i}\frac{1}{\bar{r}}\frac{\partial}{\partial\bar{r}}\left(\bar{r}\ \hat{\mu}_{eff}\frac{\partial\hat{u}}{\partial\bar{r}}\right) \tag{6b}$$

Energy:

$$\hat{\rho}\hat{u}\frac{\partial \bar{i}}{\partial \bar{x}} + 2\hat{\rho}\hat{v}\frac{\partial \bar{i}}{\partial \bar{r}} = \frac{4}{Re_i\, Pr_i}\frac{1}{\bar{r}}\frac{\partial}{\partial \bar{r}}\left(\bar{r}\frac{\hat{k}_{eff}}{\hat{c}_p}\frac{\partial \bar{i}}{\partial \bar{r}}\right) \tag{6c}$$

Integral continuity:

$$\int_0^1 \hat{\rho}\hat{u}\,\bar{r}d\bar{r} = 1/2 \tag{6d}$$

Idealizations implied by these forms are (a) the axisymmetric boundary layer approximations, (b) steady flow at low velocities, (c) constant mixture concentration, and (d) negligible axial conduction. The circumflex (^) represents non-dimensionalization with respect to the value of the quantity of the entrance.

Gas properties may be idealized as

$$\hat{\rho} = \hat{p}/\hat{T}; \quad \hat{\mu} = \hat{T}^a; \quad \hat{k} = \hat{T}^b; \quad \hat{c}_p = \hat{T}^d \tag{7}$$

Initial conditions are specified and boundary conditions are the no-slip, impermeable wall with the observed wall heat flux variation specified.

The effective viscosity is predicted with a combination of the van Driest mixing length [1956] and Reichardt middle law [1951],

$$\ell_{vD} = \kappa y \left\{1 - \exp(-y^+/y_\ell^+)\right\} \tag{8a}$$

and

$$\varepsilon_m = \varepsilon_{vD} \cdot \left(2 - \frac{y}{r_w}\right) \cdot \left[1 + 2\left(\frac{r}{r_w}\right)^2\right]/6 \tag{8b}$$

The wall temperature is used to evaluate properties in y^+. With $\kappa = 0.4$ and $y_\ell^+ = 26$, this representation yields adiabatic friction factors within about one percent of the Drew, Koo and McAdams correlation [1932] over the range $3 \times 10^4 < Re < 3 \times 10^5$.

The program uses implicit algebraic equations to represent the governing equations. These equations are iterated at each axial step to treat their coupling and the non-linear terms. Mesh spacing is chosen to provide Nusselt numbers and friction factors within about two percent of their converged values. The node nearest the wall falls at $y^+ \tilde{\leq} 0.5$ or less.

For predictions under the constant property idealizations the exponents a, b and d are set to zero and $\hat{\rho}$ is taken as unity. Then if the inlet condition is a fully developed flow, only the energy equation is solved.

Heat transfer results for fully established conditions with constant properties are shown in Figure 2. Reynolds analogy, $Pr_t = 1$, has been assumed here. Normalization by the Dittus-Boelter correlation (2) shows that such correlations may be expected to fail as the Prandtl number is reduced and the Reynolds number is increased. The two correlations would overpredict the Nusselt number with the Colburn analogy, used by Vanco [1965], being about fifteen percent worse than the Dittus-Boelter correlation for helium-argon mixtures. Whether Reynolds analogy and these numerical predictions are adequate must be determined by experiment.

2.4. Experiment

The experimental apparatus, arrangement, and procedure were similar to those used by Campbell and Perkins [1968]. Instead of a square duct, a circular tube of Hastelloy-X was used as the test section. This

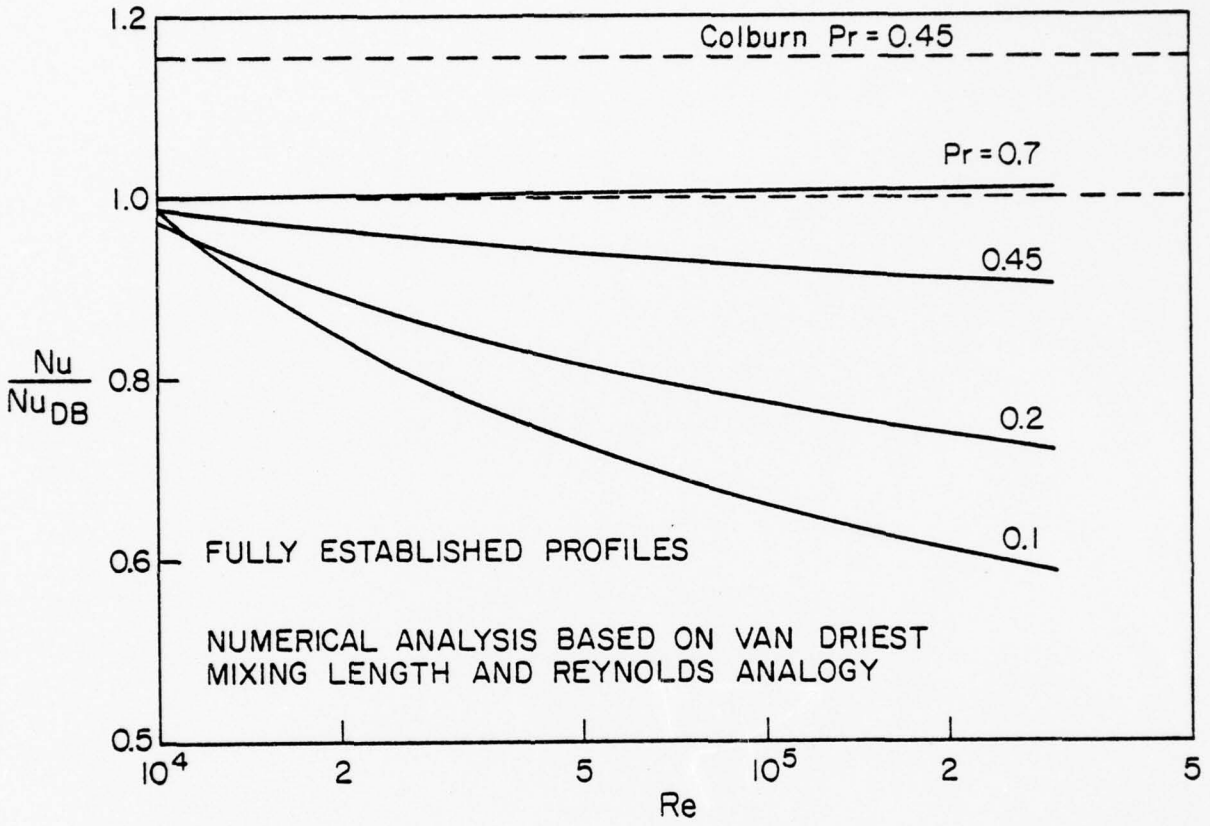

Figure 2. Heat Transfer Predictions for Fully Established Conditions. Constant Fluid Properties.

vertical tube had an inside diameter of 0.312 cm (1/8 in) and a wall thickness of 0.056 cm (0.022 in). The test section consisted of a heated section 98 diameters in length preceded by an unheated section 92 diameters in length. The unheated section ensured that the velocity profile approached fully developed flow prior to heating. Electrical resistance heating of the test section yielded an axial heat flux distribution which exponentially approached a constant value within three diameters and then remained constant within a few percent. Two pressure tapes were used. One was located in the lower electrode and the other eight diameters below the upper electrode.

Sixteen premium grade Chromel-Alumel thermocouples, 0.013 cm. (0.005 in) diameter, were spot welded to the heated section of the tube using the parallel junction suggested by Moen [1960]. Thermocouple conduction error was calculated from the heat loss calibration data and a relation developed by Hess [1965]; the thermocouple conductance was estimated from the emissivity of the bare wires and a natural convection correlation for small Rayleigh numbers. The correction is of the order of one percent of the difference between the tube temperature and the environmental temperature; at $Re \tilde{>} 3 \times 10^4$, the effects are approximately 1½ to 2 percent on the Nusselt number and 3 to 4 percent on the deduced turbulent Prandtl number.

With the exception of air, the gas was supplied in commercial gas cylinders. The manufacturer, Matheson Gas Products Division, provided the mixtures to our specifications in lots of four bottles. For the first two batches concentration was determined by gas chromotography; samples of the

same mixture varied by two percent by volume so adiabatic friction factor measurements were used to confirm the concentration selected. For the last two batches Matheson determined the concentration with a thermal conductivity column with sample variation to within 0.8 and 0.4 percent (however, the experimental uncertainty of the technique is estimated as two percent); these concentrations were also confirmed by the adiabatic friction data.

To measure the higher flow rates, our positive displacement meter was replaced by a Meriam laminar flow element. The latter was calibrated to measure the flow rate within $\pm$ 1.5 percent. Heise gages, inclined water manometers, and vertical mercury or water manometers were used to measure static pressure and pressure drop.

Table 1 summarizes the range of variables covered in this investigation. A more detailed discussion of the experiment and tabulations of the data are available in a report by Pickett [1976].

The experimental uncertainties were estimated by the method of Kline and McClintock [1953]. Typical values for the Nusselt number are 13 percent at $x/D \tilde{\sim} 1.2$ decreasing to 4 percent at $x/D \tilde{\sim} 25$ for low heating rates and slightly less for the higher heating rates. The dominant uncertainty is in the bulk stagnation temperature which depends on the mass flow rate, electrical power and the heat loss calibration.

The test section was a bare tube surrounded by a draft shield so heat loss was by radiation and natural convection. The heat loss was calibrated as a function of axial position and temperature from measurements without internal flow. During runs with flow the fraction of power dissipated to the environment, instead of to the internal gas flow, increases

Table 1. Range of Variables in the Present Experiment

	Air	Helium	Helium-Argon
Experimental Runs	25	4	28
Molecular Weight	28.97	4.003	15.3 - 29.7
Inlet Bulk Reynolds Number	32,900-100,000	30,200	31,200-102,000
Exit Bulk Reynolds Number	19,900- 89,000	18,400-26,600	17,000- 68,000
Inlet Bulk Prandtl Number	0.719	0.667	0.419-0.486
Exit Bulk Prandtl Number	0.682	0.667	0.426-0.495
Maximum T_w/T_b	1.90	1.75	1.82
Maximum T_w (°K)	817	789	828
Maximum q+	0.0027	0.0027	0.0032
Maximum Gr/Re_i^2	8.90×10^{-5}	4.84×10^{-5}	3.22×10^{-3}
Maximum Mach Number	0.26	0.25	0.33
x/D for Local Bulk Nusselt Numbers	2.1 - 82.1	2.1 - 82.1	2.1 - 82.1

with axial position and temperature level and decreases with Reynolds number. For the helium-argon data the worst situation in the present data occurred at $Re_i \tilde{\sim} 3.1 \times 10^4$ and $\tilde{M} = 29.7$ where q''_{loss}/q''_w reached 0.15 at the highest heating rate; thus, for this condition a ten percent uncertainty in heat would cause less than two percent uncertainty in the heat flux to the gas. For mixtures with lower molecular weights, improved convective heat transfer led to lower heat loss ratios, e.g., $(q''_{loss}/q''_w) \tilde{\sim} 0.07$ with $\tilde{M} = 15.3$ at the same conditions.

Adiabatic friction factors were measured before each series of heated runs. These results were used as a check of the measurements of pressure, mixture molecular weight, and flow rate. The measured friction factors were compared to the experimental correlation of Drew, Koo, and McAdams [1932],

$$f_{DKM} = 0.0014 + 0.125\ Re^{-0.32} \tag{9}$$

Figure 3 shows the measured friction factors plotted as a function of Reynolds number. Air and helium data points are included for comparison. All the measured values are within four percent of correlation (9), and three-quarters are within two percent. The data for the mixture with $\tilde{M} = 15.83$ and for helium show the best agreement. No systematic variation with molecular weight seems evident.

2.5 Heat Transfer With Constant Properties

In order to deduce the turbulent Prandtl number without complications introduced by its possible variation with heating rate, the measurements were extrapolated to the constant property idealization by the approach of Malina and Sparrow [1964]. For this method, a series of experi-

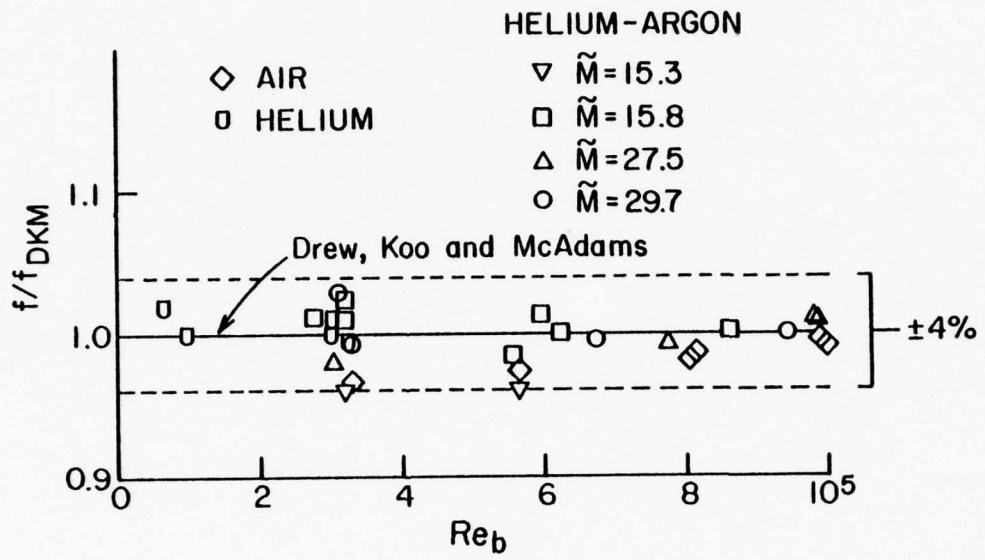

Figure 3. Comparison of Adiabatic Friction Factors to Drew, Koo and McAdams Correlation for Air, Helium and Helium-Argon Mixtures.

mental runs are taken with the same inlet Reynolds number and gas composition but with successively higher heating rates. At each thermocouple location the measured Nusselt numbers are plotted versus the local temperature difference, $T_w - T_b$. An extrapolation to $T_w - T_b = 0$ yields the deduced Nusselt number for constant property conditions, Nu_{cp}. A comparable extrapolation of the experimental uncertainty provides an estimate of the validity of these data. For the range of data reported the uncertainty in constant properties Nusselt number varied from nine percent at small axial distances to about five percent at large distances.

For fully developed conditions with air or helium as the fluid, the ratio Nu_{cp}/Nu_{DB} varied from 0.94 to 1.0 without any evident dependence on Reynolds number. With helium-argon mixtures of Prandtl number 0.42 to 0.49 the ratio varied from 0.83 to 0.93. This reduction in the normalized value corresponds to the trend predicted in Figure 2. Since the reduction is greater than predicted by the analysis, it is a first indication that a turbulent Prandtl number greater than unity may be appropriate for the mixtures.

In addition to equations (1) and (2), several other correlations have been recommended for heat transfer to gases with fully established temperature profiles downstream in tubes. Kays [1966] recommends the relation

$$Nu = 0.022\ Re^{0.8} Pr^{0.6} \tag{10}$$

for the range $0.5 < Pr < 1.0$ for the thermal boundary condition of a constant wall heat flux. This analytical correlation agreed with the present mixture data within six percent so it can be considered valid to $Pr = 0.42$;

at Pr $\tilde{}$ 0.7 it shows slightly better agreement than the Dittus-Boelter correlation (2)

Sleicher and Rouse [1975] suggested a correlation for the ranges $0.1 < Pr < 10^5$ and $10^4 < Re < 10^6$,

$$Nu_b = 5 + 0.015\, Re_f^m\, Pr_w^n \tag{11}$$

where

$$n = (1/3) + 0.5 \exp(-0.6\, Pr_w)$$

and

$$m = 0.88 - 0.24/(4 + Pr_w)$$

The subscripts, b, f and w, refer to evaluation of properties at bulk, film and wall temperatures, respectively, when property variation is significant. For constant properties in the range of the present data this relation predicts lower values than the simpler correlation of Kays. At Pr $\tilde{}$ 0.7 the predictions of Sleicher and Rouse correspond to the lower limit of the data and at Pr $\tilde{}$ 0.45 they are a few percent below the lower limit of these data. While the magnitudes differ from the data slightly, their trend with Prandtl number corresponds to the present predictions and measurement.

In order to deduce the turbulent Prandtl number the technique of McEligot, Picket and Taylor [1976] is applied. Essentially, hypothesized distributions $Pr_t(y)$ are introduced in the numerical analysis and the predicted Nusselt numbers, Nu(x), are compared to the data, $Nu_{cp}(x)$. Variations in the shape of $Pr_t(y)$ are reflected in variation in the shape of Nu(x) in the thermal entry region. One of the main advantages of this matching technique is that it concentrates on determining Pr_t accurately in the

region which is most important for predicting surface temperatures in flows heated from the wall.

In this study, as in the demonstration by McEligot, Pickett and Taylor [1976], the experimental uncertainty at small axial distances was too large to determine $d\,Pr_t/d(y/r_w)$ clearly. Consequently, a constant value of Pr_t was used in the present calculations; their sensitivity tests showed that it is essentially equivalent to an effective $Pr_{t,w}$ for the wall region. Only results for x/D greater than eight were used to determine $Pr_{t,w}$.

Figure 4 illustrates examples of the comparisons between measured $Nu_{cp}(x)$ and predicted Nu(x) used to determine $Pr_{t,w}$. Examples for three Reynolds numbers and two Prandtl numbers are shown. Brackets indicating the estimated experimental uncertainties of the $Nu_{cp}(x)$ are also included.

Figure 4a shows the measured and calculated Nu_{cp} for a helium-argon mixture with a molecular weight of 15.3, Prandtl number of 0.42, and Reynolds number of 32,000. The turbulent Prandtl number is seen to be about 1.1 or slightly less. From comparisons on similar graphs, $Pr_{t,w}$ was estimated to be 1.1 ± 0.1 for helium-argon mixtures with molecular weights of approximately 15, Prandtl numbers of 0.42, and Reynolds numbers between 32,000 and 55,200. Measurements and predictions are shown in Figures 4b and 4c for a helium-argon mixture at a molecular weight of 29, Prandtl number of 0.486, and Reynolds numbers of 31,600 and 82,100. From similar graphs, $Pr_{t,w}$ was estimated to be 1.0 ± 0.1 for the range of helium-argon mixtures with molecular weights between 27 and 30, Prandtl numbers between 0.46 and 0.49, and Reynolds numbers between 31,600 and 102,000.

The effect of Reynolds number on $Pr_{t,w}$ can be examined qualitatively using the results in Figure 4b and 4c, but the experimental uncertainty

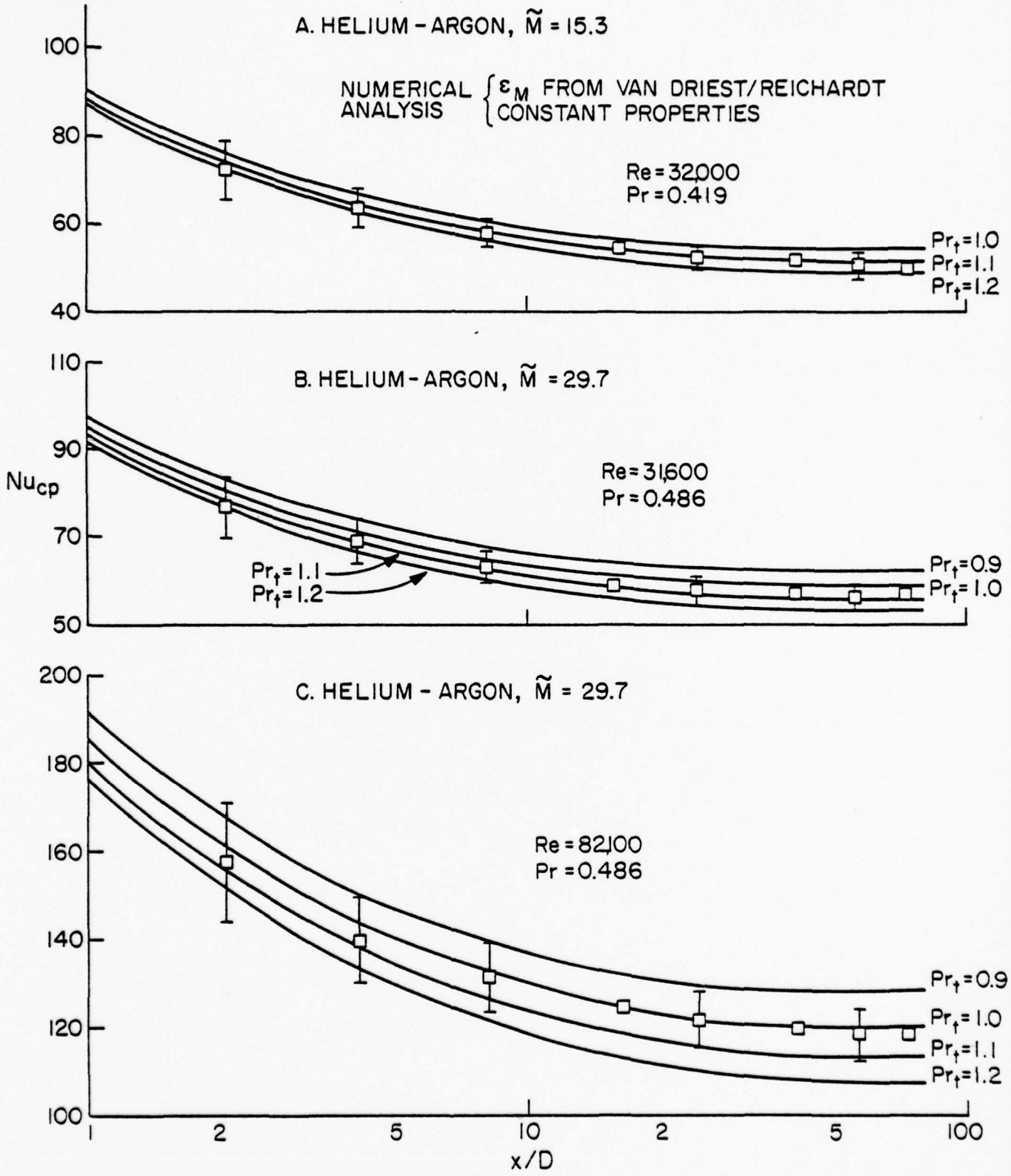

Figure 4. Examples of the Comparisons Between Measured $Nu_{cp}(x)$ and Predicted $Nu(x)$ as Used to Deduce Pr_{tw} for Constant Properties.

prohibits a quantitative determination. These results are for the same Prandtl number (Pr = 0.486), but two different Reynolds numbers: 31,600 and 82,100. For x/D greater than eight, and at the lower Reynolds number, the measured $Nu_{cp}(x)$ data are slightly below the calculated Nu(x) curve for a $Pr_{t,w}$ of 1.0. At the higher Reynolds number and same axial locations, the measured $Nu_{cp}(x)$ are slightly above the prediction for $Pr_{t,w} = 1.0$. For the stated conditions, it appears that $Pr_{t,w}$ may have a weak dependence on Reynolds number, and may decrease slightly as the Reynolds number increases.

The effect of molecular Prandtl number on turbulent Prandtl number can be examined using the observations from Figures 4a and 4c which are summarized in Table 2. The air data of McEligot, Pickett and Taylor [1976] can also be considered since the present study shows $Pr_{t,w}$ to vary only slightly with Reynolds number. For the range shown in Table 2, $0.42 < Pr < 0.7$, the turbulent Prandtl number increases as the molecular Prandtl number decreases as suggested by the review of A. J. Reynolds [1975]. However, reference to Figure 4 shows that predictions based on O. Reynolds' analogy are still valid to within five to ten percent which is adequate for many engineering applications.

2.6 Heating with Property Variation

In order to increase power densities or lower the weight of closed Brayton cycle systems, moderately high heating rates must be employed. Consequently, the temperature-dependence of the fluid transport properties causes significiant variation in properties appearing in the coefficients of equations (6) and coupling of the equations. The results and correlations

Table 2. Variation of $Pr_{t,w}$ with Respect to Molecular Prandtl Number

Gas	Molecular Weight	Prandtl Number	$Pr_{t,w}$	Reynolds Number
Helium-argon	15.3	0.419	1.1 ± 0.1	32,000
Helium-argon	29.7	0.486	1.0 ± 0.1	31,600
Air*	28.97	0.72	0.9 ± 0.1	44,500

*McEligot, Picket and Taylor, [1976].

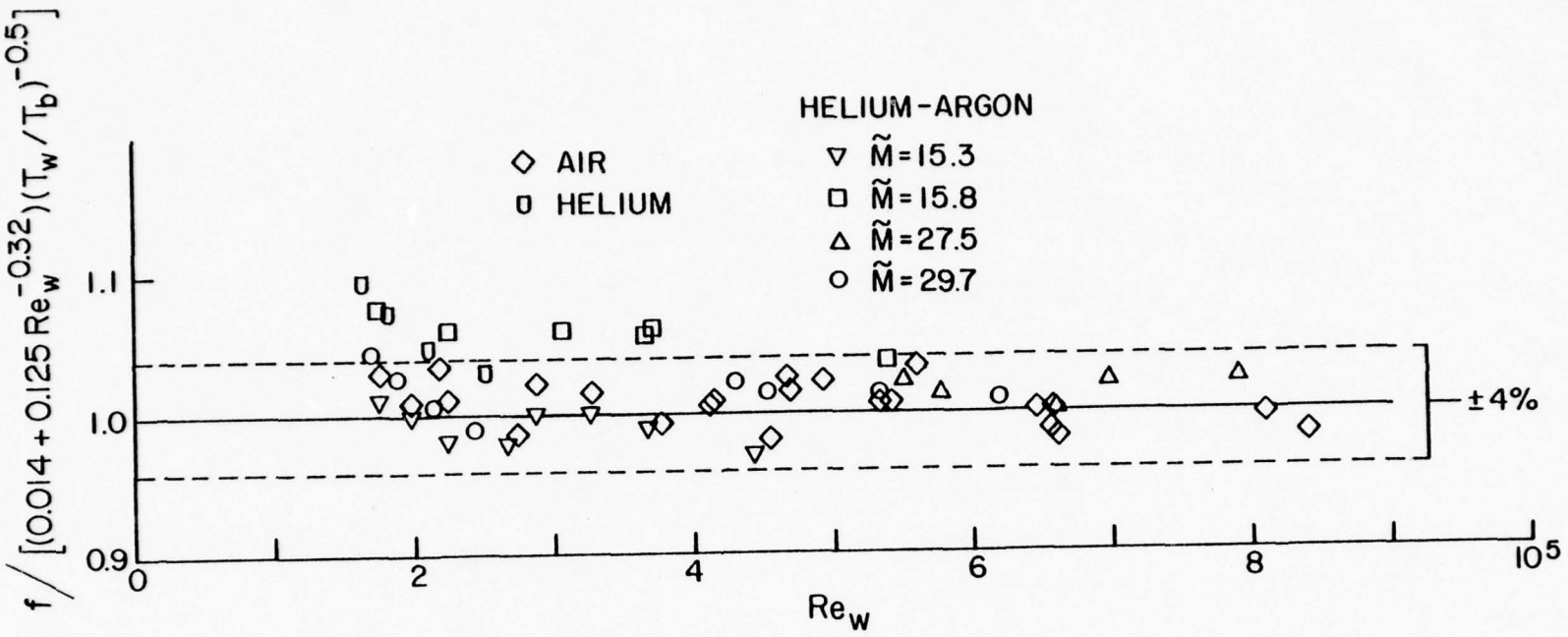

Figure 5. Comparison of Average Friction Factors to Taylor Variable Properties Correlation for Air, Helium and Helium-Argon Mixtures.

based on the constant property idealizations become invalid. In this section the modifications accounting for property variation are examined and the application of the turbulent Prandtl number, determined above for constant properties, is tested.

Since only two pressure taps were attached to the test section, local friction factors could not be determined. Overall average friction factors with heat addition were compared to the correlation proposed by Taylor [1976]

$$f_{av} = (0.0014 + 0.125\ Re_w^{-0.32})\ (T_{w,av}/T_{b,av})^{-0.5} \qquad (12)$$

for the data of a wide variety of experiments with gas flow. Most previous measurements agreed within ten percent. For evaluation of this expression, arithmetic averages of the conditions at the two pressure taps were used to calculate the average temperatures and pressure and, hence, density and viscosity. The overall friction factor was determined from the frictional pressure drop,

$$\Delta p_{fr} = p_1 - p_2 - \frac{G^2 R}{g_c}\left(\frac{T_{b2}}{p_2} - \frac{T_{b1}}{p_1}\right)$$

and the modified wall Reynolds number was defined as

$$Re_w = (GD/\mu_w)(T_{b,av}/T_{w,av}).$$

In the present study correlation (12) predicted most of the data within four percent; all are within ten percent. These measurements are presented in Figure 5. Comparison to Figure 3--which uses the constant properties limit of the same equation--shows a general increase in the normalized data with heating. This increase indicates the exponent on the

temperature ratio may be slightly too large, leading to an underprediction of the average wall friction. The effect appears to be most significant for the lower molecular weight mixtures in low Reynolds number flow.

The downstream measurements of the local Nusselt number were compared to correlation (11) of Sleicher and Rouse [1975]. Though intended to account for property variation, the values predicted were 15 to 40 percent lower than the measurements for the mixtures. Thus, this correlation could yield excessively conservative estimates of surface temperatures in design calculations.

Magee [1968] has suggested accounting for property variation and thermal entry development by applying a multiplicative factor to the constant property correlation. In the range, $2.1 < x/D < 81.6$, his correlation predicted 97 percent of our data for heat transfer to air and helium to within 10 percent. Since the transport properties of helium-argon mixtures vary with temperature in approximately the same manner as for air and helium, the same exponent was taken for the temperature ratio. Kays [1966] discusses the effect of Prandtl number variation on the thermal entry behavior for circular tubes. As the Prandtl number decreases the thermal entry region is expected to become more pronounced, so a larger coefficient is appropriate for the axial development term. These considerations plus a correlation of the constant properties results [Pickett, 1976] lead to

$$Nu_b = 0.021\ Re_b^{0.8}\ Pr_b^{0.55}\ [(T_w/T_b)^{-0.4} + 0.85\ D/x] \qquad (13)$$

which predicts 92 percent of the present helium/argon data to within ten percent for the range $2.1 < x/D < 81.6$. The greatest discrepancy occurs in the range $4 \leq x/D \leq 16$ at high heating rates; in this situation the measurements are underpredicted by 5 to 15 percent.

The validity of the deduced values of the turbulent Prandtl number were tested for the conditions of two experimental runs, one with slight property variation and the other with strong heating. Both runs were with the same mixture with $\tilde{M} = 29.7$ and $Pr \tilde{\sim} 0.49$ and essentially the same inlet Reynolds number. For predictions the measured wall heat flux distribution was used for the thermal boundary condition and exponents in equations (5) were taken as $a = 0.772$ and $b = 0.741$ to account for property variation. From the constant property results the turbulent Prandtl number was taken as 1.02.

Comparisons between the two heating rates and the numerical predictions are presented as Figure 6. These demonstrate that the combined effect of the strong heating rate and the property variation is a reduction in Nu_b of about 1/3 in the downstream region. The difference in Nu decreases as the thermal entry is approached while the temperature ratio peaks near ten to fifteen diameters, the region where correlation (13) shows the greatest discrepancy.

The numerical predictions and data agree well for both heating rates. This observation is to be expected for the lower heating rate, $q^+ = 0.0006$, since the maximum difference between wall and bulk properties was about eleven percent. Thus, the conditions did not differ substantially from the constant properties idealization under which the turbulent Prandtl number was deduced.

At the higher heating rate, $q^+ = 0.0032$, the property variation at a cross section approaches sixty percent. Thus, it is reasonable to ask whether the heating causes a significant effect on the turbulent Prandtl number in the important wall region. Apparently, it does not. Applying

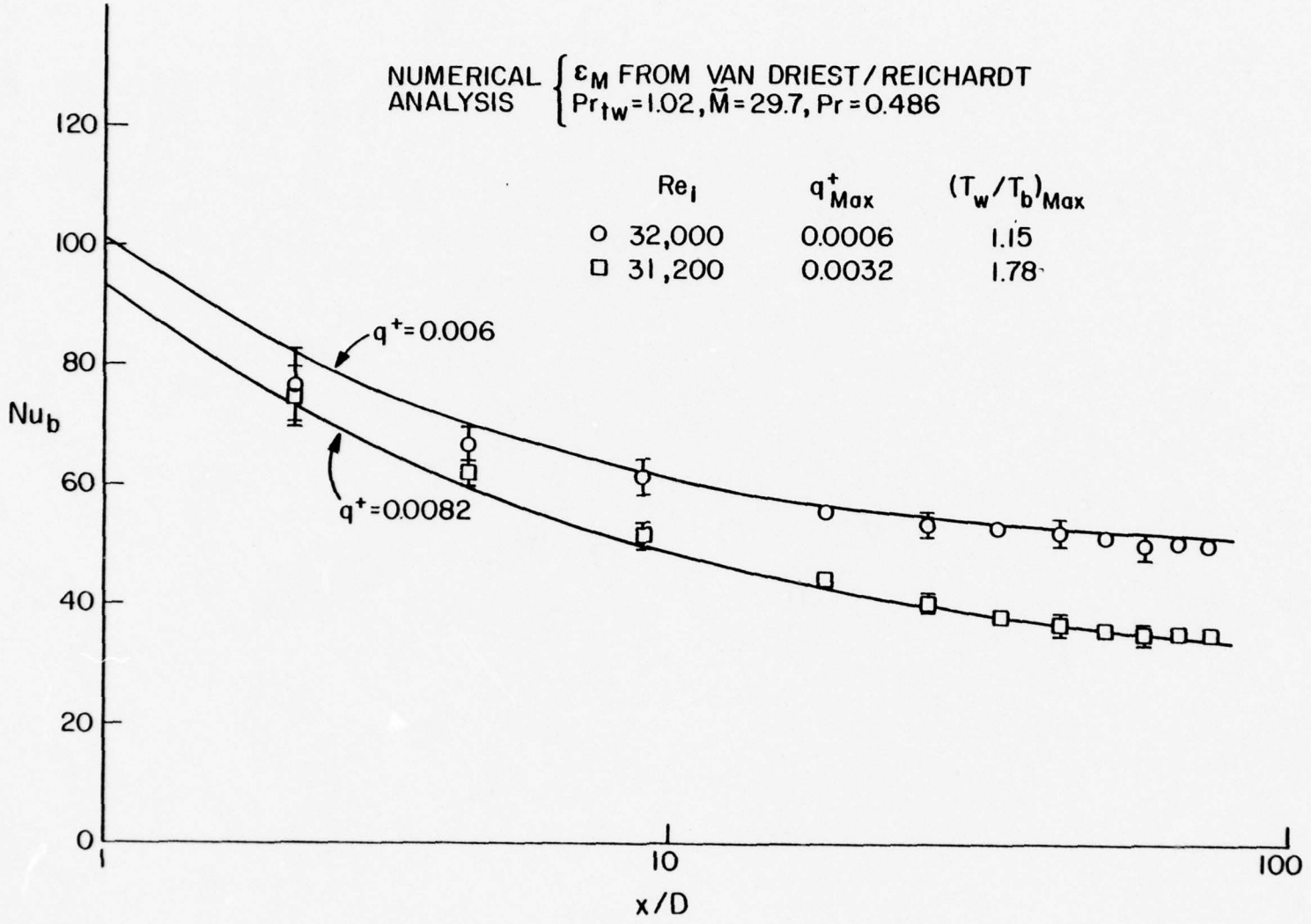

Figure 6. Comparison of Data to Numerical Predictions Accounting for Transport Property Variation.

the value deduced for constant properties leads to close agreement between predicted and measured Nusselt numbers at this heating rate as well (Figure 6). While not an exhaustive examination, this test is an initial indication that Pr_t is not a strong function of heating rate. Extension to other molecular Prandtl numbers, Reynolds numbers and heating rates is the subject of further work now in progress.

3. NUMERICAL PREDICTION OF WALL FRICTION IN LAMINAR FLOW WITH PROPERTY VARIATION

3.1. Background

In gas turbine cycles the regenerative heat exchanger is typically constructed of parallel plates, with short fins attached forming additional parallel surfaces. Consideration of the heat transfer performance versus pumping power requirements of these heat exchangers usually results in design for operation in the laminar or transitional flow regime. For laminar flow heat exchangers, the streamwise length of the fins is shortened in order to take advantage of the increased heat transfer coefficient of developing boundary layers by continually reinitiating the boundary layer. The thermal boundary condition is an approximately constant wall heat flux. As a guide to the effects of mixture composition and property variation in such geometrics, the present work - for a first objective - investigates the simultaneous development of laminar thermal and velocity boundary layers in the entry region of parallel plate ducts.

The previous report [Taylor et al., 1976] (a) briefly discussed related work which can be extended to provide improved guidance to the designer of regenerative heat exchangers for mixtures of noble gases,

(b) summarized pertinent knowledge of their transport properties and demonstrated the generalizations possible to reduce the analytical task, (c) outlined the numerical solution of the governing equations, and (d) presented the heat transfer results of interest in design in terms of lengthwise mean parameters. The numerical results are summarized in the present report as Table 3. The mean Nusselt number, evaluated in terms of properties evaluated at the average bulk temperature, could be approximated as

$$Nu_a = [8.235^2 + 1.931^2/(Pr^{0.254}L^*)]^{1/2} \qquad (14)$$

This equation is of the order of five percent lower than the numerical prediction near $L^* = 0.01$. For moderate heating rates it would be within about ten percent of the numerical results and would be low; in heat exchanger design this would lead to units slightly longer than necessary. Alternatively, the constants in equation (14) could be optimized for another range at the expense of the accuracy of predictions in the immediate entry. It was found that the use of properties evaluated at the average film temperatures did not collapse the variable properties predictions to the constant properties result as well as the bulk temperature did.

3.2. Prediction of Wall Friction with Property Variation

While most analyses presently available for developing flows present friction results in terms of the wall shear stress evaluated from the velocity gradient at the wall (f_s), this approach is not of use to the designer when the velocity profile is changing substantially, as in the entry or when a gas is heated. To predict the required pressure drop with a one-dimensional

Table 3. Local and Mean Parameters for Laminar Forced Convection Between Parallel Plates.

$\frac{4x}{D_h Pr Re_0}$	T_b/T_0	T_w/T_b	Nu_{bx}	$\frac{f \cdot Re_{bx}}{24}$	T_{wa}/T_{ba}	Nu_{ba}	$\frac{f_{ba} \cdot Re_{ba}}{24}$	$\frac{p_0 - p}{G^2/(2g_c \rho_0)}$
				$Pr = 0.2$				
				$Q^+ = 100$				
0.001	1.10	3.12	40.1	19.5	2.11	74.2	34.3	—
0.0023	1.23	3.50	27.9	11.8	2.38	49.9	22.4	—
0.0055	1.55	3.48	18.8	7.38	2.50	32.7	13.2	—
0.01	2.00	3.09	14.3	6.05	2.39	24.1	9.41	—
0.023	3.30	2.19	10.4	4.51	1.92	15.7	6.46	—
0.055	6.50	1.42	9.08	2.20	1.36	11.0	3.76	—
0.01	11.0	1.18	8.61	1.53	1.16	9.51	2.42	—
0.02	21.0	1.06	8.36	1.27	1.06	8.58	1.76	—
				$Q^+ = 10$				
0.001	1.01	1.27	39.9	12.3	1.12	75.3	22.0	0.127
0.0023	1.02	1.35	27.4	8.63	1.18	51.0	15.2	0.217
0.0055	1.06	1.48	19.0	5.90	1.25	34.2	10.3	0.395
0.01	1.10	1.56	15.1	4.52	1.29	26.2	7.84	0.611
0.023	1.23	1.61	11.4	3.24	1.34	18.4	5.34	1.18
0.055	1.55	1.49	9.40	2.37	1.30	13.2	3.59	2.56
0.1	2.00	1.33	8.93	1.93	1.22	11.1	2.76	4.72
0.2	3.00	1.17	8.60	1.51	1.13	9.61	2.09	10.9
0.5	6.00	1.05	8.36	1.17	1.05	8.61	1.52	43.8
				$Q^+ = 0$, constant properties				
0.001	—	—	40.1	10.3	—	75.7	19.4	—
0.0023	—	—	27.5	6.64	—	51.3	12.9	—
0.0055	—	—	18.9	4.38	—	34.4	8.46	—
0.01	—	—	14.9	3.28	-	26.4	6.33	—
0.023	—	—	11.2	2.26	—	18.7	4.25	—
0.055	—	—	9.14	1.58	—	13.6	2.85	—
0.1	—	—	8.55	1.28	—	11.4	2.20	—
0.2	—	—	8.32	1.07	—	9.92	1.67	—
0.5	—	—	8.24	1.00	—	8.92	1.28	—
				$Q^+ = -2$				
0.001	1.00	0.950	40.1	9.46	0.975	75.7	18.8	0.0863
0.0023	1.00	0.927	27.5	6.21	0.963	51.4	12.4	0.128
0.0055	0.99	0.892	18.9	3.95	0.946	34.5	8.00	0.188
0.01	0.98	0.861	14.9	2.83	0.931	26.5	5.90	0.239
0.023	0.95	0.805	11.2	1.83	0.905	18.7	3.86	0.318
0.055	0.89	0.725	8.92	1.14	0.871	13.6	2.50	0.379
0.09	0.82	0.655	8.21	0.792	0.845	11.7	1.97	0.362
				$Pr = 0.4$				
				$Q^+ = 100$				
0.001	1.10	3.25	37.7	14.0	2.18	69.1	25.2	0.464
0.0023	1.23	3.65	26.4	9.34	2.46	46.7	16.6	0.900
0.0055	1.55	3.60	17.9	6.26	2.58	30.8	10.4	1.94
0.01	2.00	3.18	13.7	4.99	2.45	22.9	7.63	3.49
0.023	3.30	2.24	10.0	3.43	1.95	15.0	5.11	8.91
0.055	6.50	1.43	8.74	1.73	1.38	10.6	2.92	26.6
0.1	11.0	1.18	8.45	1.34	1.16	9.19	1.97	63.7
0.2	21.0	1.06	8.31	1.21	1.06	8.41	1.60	247.

Table 3.--continued

$\frac{4x}{D_h Pr Re_0}$	T_b/T_0	T_w/T_b	Nu_{bx}	$\frac{f \cdot Re_{bx}}{24}$	T_{wa}/T_{ba}	Nu_{ba}	$\frac{f_{ba} \cdot Re_{ba}}{24}$	$\frac{p_0 - p}{G^2/(2g_c\rho_0)}$
				$Pr = 0.4$				
				$Q^+ = 0$, constant properties				
0.001	—	—	36.9	7.12	—	69.5	13.9	0.133
0.0023	—	—	25.5	4.75	—	47.2	9.22	0.204
0.0055	—	—	17.6	3.16	—	31.8	6.05	0.319
0.01	—	—	14.0	2.39	—	24.5	4.55	0.436
0.023	—	—	10.7	1.69	—	17.4	3.09	0.682
0.055	—	—	8.80	1.24	—	12.8	2.11	1.12
0.1	—	—	8.35	1.07	—	10.9	1.67	1.61
0.2	—	—	8.25	1.01	—	9.57	1.35	2.59
0.5	—	—	8.24	1.00	—	8.77	1.14	5.47
				$Pr = 2/3$				
				$Q^+ = 100$				
0.0013	1.13	3.51	32.1	10.1	2.33	57.7	17.1	0.657
0.0023	1.23	3.76	25.3	7.79	2.52	44.3	13.1	1.04
0.0055	1.55	3.70	17.3	5.41	2.64	29.4	8.55	2.25
0.01	2.00	3.24	13.3	4.32	2.50	21.9	6.42	4.09
0.023	3.30	2.27	9.73	2.85	1.98	14.5	4.30	10.7
0.055	6.50	1.44	8.58	1.52	1.38	10.28	2.47	33.1
0.1	11.0	1.18	8.38	1.27	1.17	9.02	1.76	85.1
0.2	21.0	1.06	8.28	1.20	1.06	8.33	1.53	373.
				$Q^+ = 10$				
0.001	1.01	1.28	34.7	6.71	1.14	65.0	12.1	0.216
0.0023	1.02	1.40	24.3	4.74	1.20	44.3	8.33	0.360
0.0055	1.05	1.53	17.1	3.39	1.27	30.0	5.71	0.638
0.01	1.10	1.62	13.7	2.72	1.32	23.1	4.43	0.975
0.023	1.23	1.66	10.6	2.09	1.36	16.5	3.16	1.87
0.055	1.55	1.52	8.88	1.62	1.32	12.1	2.26	4.16
0.1	2.00	1.35	8.53	1.41	1.23	10.3	1.84	8.03
0.2	3.00	1.18	8.37	1.27	1.13	9.12	1.55	21.0
0.5	6.00	1.05	8.29	1.11	1.05	8.40	1.33	112.
				$Q^+ = 0$, constant properties				
0.0013	—	—	30.9	4.82	—	57.7	9.52	0.198
0.0023	—	—	24.1	3.71	—	44.3	7.20	0.265
0.0055	—	—	16.8	2.50	—	30.0	4.74	0.417
0.01	—	—	13.4	1.93	—	23.2	3.58	0.573
0.023	—	—	10.3	1.40	—	16.6	2.46	0.906
0.055	—	—	8.64	1.09	—	12.3	1.73	1.52
0.1	—	—	8.29	1.01	—	10.6	1.42	2.27
0.2	—	—	8.24	1.00	—	9.40	1.21	3.87
0.5	—	—	8.24	1.00	—	8.70	1.08	8.67
				$Q^+ = -2$				
0.001	1.00	0.942	34.7	5.26	0.971	65.2	10.5	0.165
0.0023	1.00	0.916	24.1	3.46	0.958	44.4	6.94	0.246
0.0055	0.99	0.878	16.7	2.26	0.939	30.0	4.50	0.371
0.01	0.98	0.845	13.3	1.69	0.923	23.2	3.35	0.488
0.023	0.95	0.787	10.2	1.15	0.896	16.6	2.25	0.704
0.055	0.89	0.709	8.43	0.807	0.863	12.3	1.52	0.994
0.09	0.82	0.647	8.01	0.681	0.841	10.8	1.25	1.17

design procedure, one uses the "apparent" friction factor, f_{ap}, based on the wall shear determined by treating the momentum change as one-dimensional. The same treatment is often employed in experiments where size prohibits velocity profile measurements. Both methods of presentation can be chosen with numerical results; consequently, Bankston and McEligot [1970] were able to demonstrate (a) the numerical values of f_s and f_{ap} can differ substantially and (b) discrepancies earlier thought to exist between experiments and analyses were primarily due to the differences in the definition used for the friction factors.

As with the heat transfer results we concentrate in presenting a mean apparent friction factor,

$$f_a = - \frac{D_h}{4L} \frac{\rho}{G^2/2g_c} \Delta_{0\,L} \{p + \frac{G^2}{\rho_b g_c}\} \tag{15}$$

(The local apparent friction factor, f_x, appearing in Table 3 is defined in the analogous derivative form with d/dx replacing $(1/L)\Delta_{0\,L}$). When $_b$ and constant, the second term in brackets does not change and the definition reduces to that of Shah and London [1971]. With constant fluid properties one solves the flow problem only, so the result is independent of Prandtl number and can be written as a single function $f_a(L^+)$ which approaches $f_a \cdot Re/24$ as L^+ becomes large. This function may be found tabulated in Table 3 or can be derived from earlier local results [Schade and McEligot, 1971; Bodoia and Osterle, 1961]. For a continuous approximation, the approach of Schlünder [1974] can be used as in the heat transfer results to give

$$f_a \cdot Re/24 = \sqrt{1 + 0.0788/L^+} \tag{16}$$

which represents the numerical results well in the immediate entry but is 4 to 5 percent high in the range, $0.05 < L^+ < 0.2$.

With varying transport properties, the energy equation is coupled to the flow equations via the temperature-dependent viscosity and density, so the wall friction also becomes a function of the Prandtl number and the heating rate. Again the question arises as to the better method of accounting for the fluid property variations. Predictions of friction are not as well behaved as heat transfer parameters. In contrast to the heat transfer results, direct use of the average bulk properties in f_a, Re and L^+ does not collapse the results nicely around the prediction based on constant properties; the main effect is to spread the curves towards larger L_{ba}^+ as Q^+ increases.

The effect of heating rate on apparent wall friction is presented in Figure 7 partially in terms of average bulk properties. That is, ρ_{ba} is used for the coefficient in equation (15) and Re_{ba} is defined as before but the non-dimensional length is based on inlet properties, i.e., L_o^+. With this representation, heating increases f_{ba}. Re_{ba} considerably more than Nu_{ba} is raised at the same level of Q^+. At lengths greater than $L^+ = 0.1$ the curves with heating approach the constant properties curve only slowly, although T_{wa}/T_{ba} is close to unity, as the heated entry continues to affect the integrated results far downstream. Close inspection of the trends for the highest heating rates shows that as Pr increases a convergence - from heated entry behavior towards agreement with constant property behavior - is moved further downstream. This effect corresponds to the thermal boundary layer and shear boundary layer as the Prandtl number changes: Nu(L*) shows only a moderate effect of Pr, so for the same heating rate the value of T_w/T_b is almost the same at equal values of L* rather than L^+, thus T_w/T_b approaches

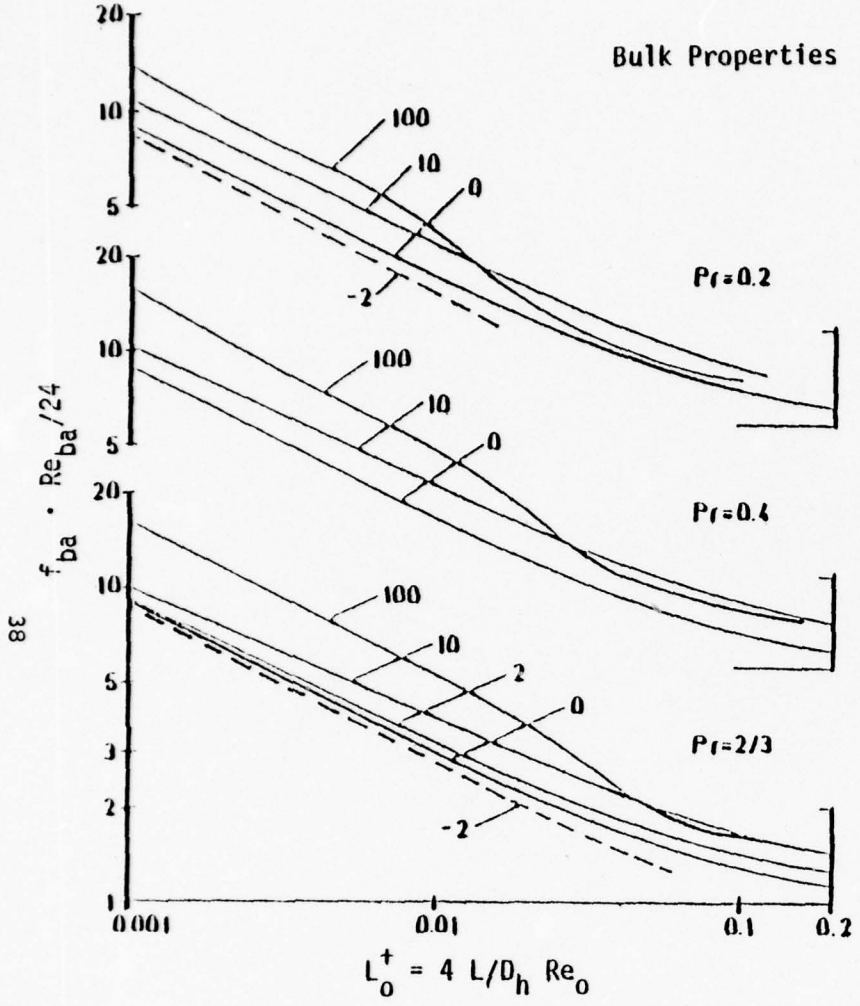

Figure 7. Mean Wall Friction Predictions in Terms of Bulk Properties.

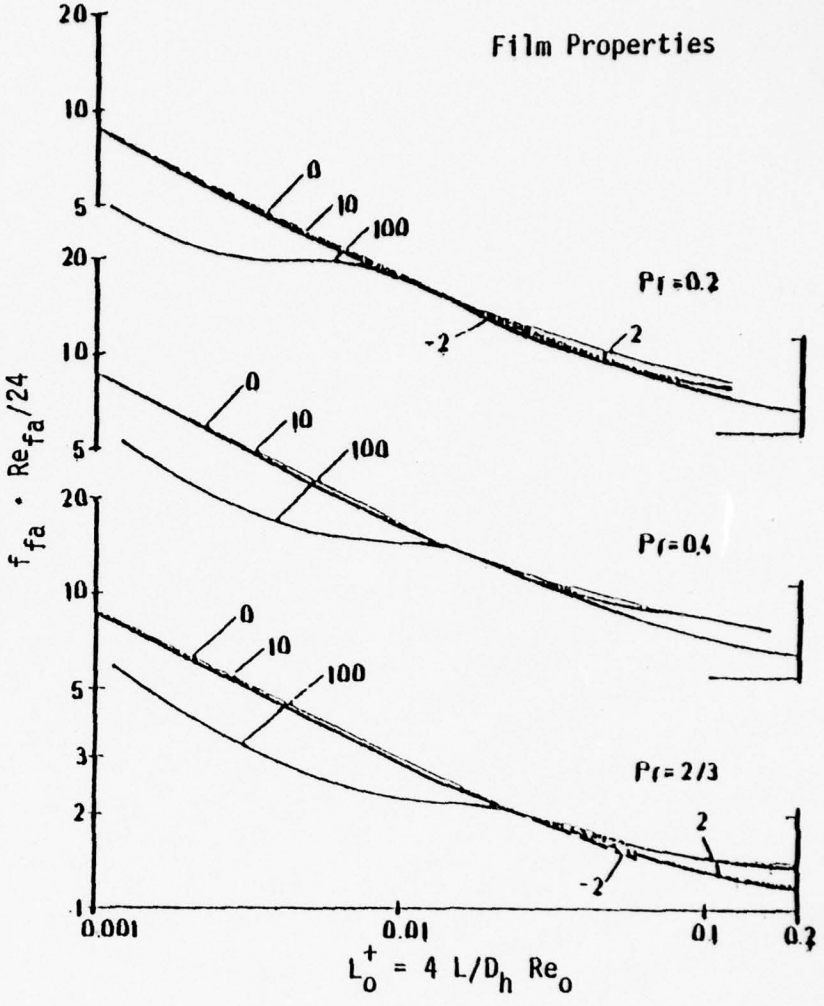

Figure 8. Mean Wall Friction Predictions in Terms of Film Properties.

unity for Pr = 0.2 at earlier values of L^+ than for Pr = 2/3 and the variation of properties across the channel is less for Pr = 0.2 at the same L^+. While the friction predictions for heating approach the adiabatic prediction as L_{ba}^+ increases, those for cooling diverge; this result also corresponds to the trend of property variation since the ratio T_{ba}/T_{wa} increases downstream for cooling as described earlier in the section on heat transfer.

As with the heat transfer results, the apparent effect of property variation on wall friction is sensitive to the choice of reference temperature. With average film temperature for the reference, the shape of the resulting curves differs from the shape with bulk temperature as reference. In Figure 8 the product $f_{fa} \cdot Re_{fa}/24$ is plotted against L_o^+; ρ_{fa} is used in the coefficient in equation (15) and Re_{fa} is based on μ_{fa}. There is no advantage in comparison on the basis of L_{fa}^+ since results are shifted then further to the right (with heating) so that for $L^+ \gtrsim 0.01$ the difference from the adiabatic prediction is increased. For heating: the friction parameters are reduced for short lengths; then the predictions converge with and across the constant properties curve and remain slightly greater at larger distances. In comparison to the bulk property predictions, the effects for short and long ducts are approximately the same magnitude with strong heating, but for intermediate lengths and for $Q^+ \lesssim 10$ a display in terms of film properties shows signicantly less variation. In the range $-2 < Q^+ < 2$ there is no significant effect of heating until L_o^+ approaches 0.1 with film properties and then the effect is only of the order of five to ten percent. As is the case for bulk properties, the convergence towards the adiabatic prediction is at successively greater distances (L_o^+) as the

Prandtl number increases, but for the same condition it is several times earlier with film properties. With cooling: the directions of the trends are reversed but for $Q^+ > -2$ they are essentially again negligible for entry problems.

It is not clear from Figure 7 and 8 which approach is better: property ratio or film temperature. The property ratio approach would be represented as

$$(f_{ba} \cdot Re(L_o^+))/(f_a \cdot Re(L_o^+))_{cp} = (T_{wa}/T_{ba})^q \qquad (17)$$

so this quotient is plotted versus temperature ratio in Figure 9 to examine the suitability of a single exponent. A complicated pattern appears. In contrast to the expectation of Kays and London [1964], the general trend is a substantial increase with temperature ratio. There are slight differences with Prandtl number but the trends are mostly the same. An exponent q of the order of unity would overpredict the friction factor at the higher temperature ratios and underpredict it at lower values. For cooling, $q = 1$ is valid within a few percent. For moderate heating, the necessary value of q (i.e., the slope of a line from the origin on this logarithmic plot) varies with length L_o^+: it is approximately constant as the temperature ratio increases with length then increases gradually as the ratio drops for successively longer ducts. The latter effect is a consequence of the slow convergence of $f_{ba} \cdot Re_{ba}$ to the adiabatic curve for long ducts as discussed earlier. It is seen that a function $q(L_o^+, Q^+, Pr)$ would be necessary to describe the detailed behavior. For $Q^+ = 2$ and $L_o^+ < 0.6$, an exponent $q = 1.5$ would reduce the difference from the constant properties curve from 13 percent to a 7 percent discrepancy. With $Q^+ = 10$, $q = 1.2$

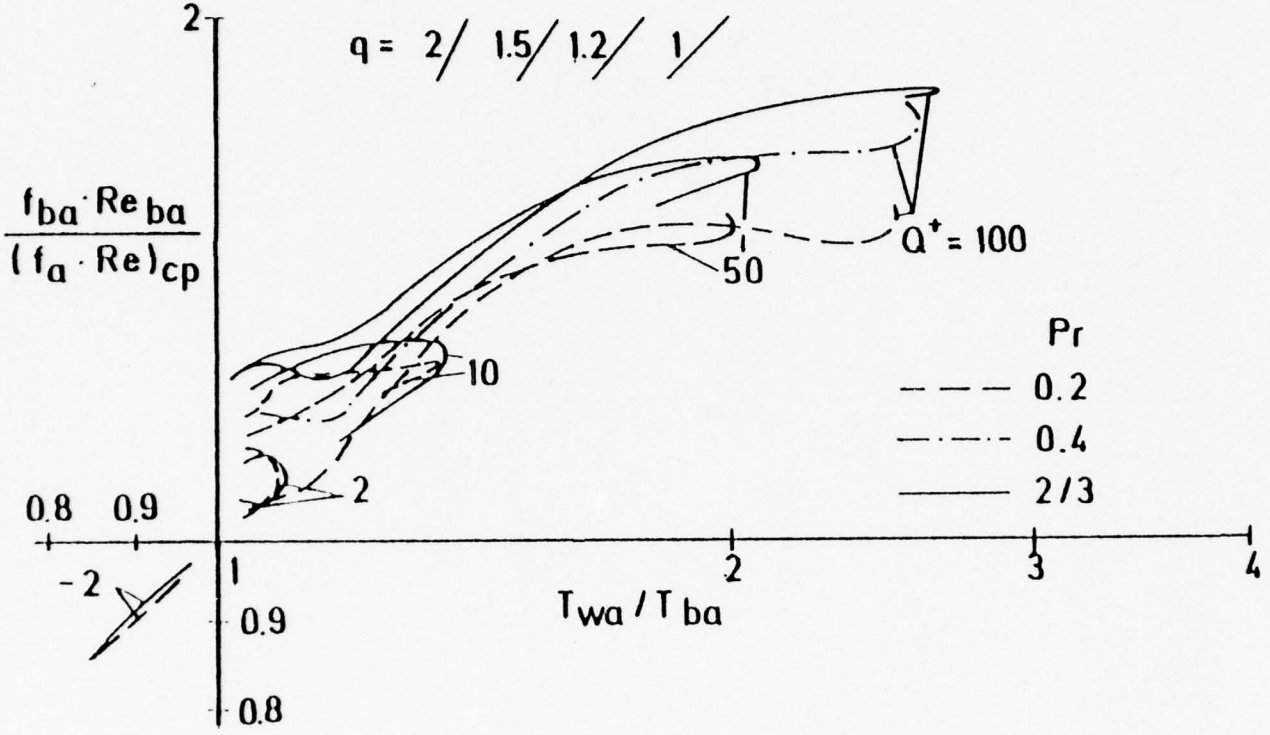

Figure 9. Examination of Property Ratio Method for Mean Wall Friction.

is a better approximation, but the discrepancy would still reach twenty percent. These comments and comparison of Figures 7 and 9 suggest that the two methods have approximately the same overall accuracy for $Q^+ \lesssim 2$ with a slight advantage to the film properties approach for short ducts. For moderate heating - to $Q^+ = 10$ - the film property method is clearly superior, while at higher heating rates both methods show regions where the simple correlations would mislead the designer substantially.

It is perhaps inconvenient for the designer to have one method perform better for heat transfer while the other is preferable for wall friction, but the difficulty should be negligible provided the present definitions of the parameters are used. Once the heat transfer problem is solved for the wall temperature using average bulk properties, the average film temperature can be calculated from the results and can then be employed to predict the wall friction behavior.

Analytical correlations such as equations (14) and (16) are useful for parameter studies of systems and for initial sizing of components when hundreds to thousands of individual configurations may be calculated. When greater accuracy is needed in final design decisions - or if variable wall heat flux should be treated - the numerical analysis can be employed directly. With the direct application of the program, the question of definitions of the non-dimensional parameters is avoided; the engineer can choose definitions to suit his own convenience, including direct presentation in temperatures, pressure and lengths in units of his choice.

4. INITIAL MEASUREMENTS WITH CLOSED LOOP

The schematic description of the closed loop for measurements with expensive gas mixtures, such as helium and xenon, has been presented by Taylor et al. [1976]. The basic loop apparatus was completed during the summer, 1976. Thermal instrumentation has been interfaced to our PDP-8M/HP3480-5 digital data acquisition system [McEligot, 1975b]. All components of this system have been received except the KL8J-A interface for direct connection to the University DEC-10/CDC 6400 system; this interface is on order. In the present configuration data stored in the PDP-8M can be transferred on DEC tape to the DEC-10 by courier. The initial data acquisition programs are in operation.

The first test section in the loop was a circular tube of 0.253 inch OD and 0.0115 inch thick walls, with 60 diameters between electrodes. Heat loss and resistivity calibrations were conducted from room temperature to over 1200°F. Adiabatic friction measurements spanned the range 35,000 < Re < 83,000 with air in order to test flow measurement techniques primarily. Preliminary tests included the following ranges:

Gas	Molecular Weight	Prandtl Number	Reynolds Number	Max-Wall Temperature	System
Argon	40.0	0.67	7,600	510°F	Closed Loop w/Diaphram Pump
Air	29.0	0.72	30,000-80,000	1010°F	Open Loop
He-Ar	31.0	0.50	40,000	230°F	Closed Loop w/Piston Pump
Air	29.0	0.72	50,000	200°F	Closed Loop w/Piston Pump

Mixtures of gases other than the noble gases are expected to provide reduced molecular Prandtl numbers as well. Since many common gases are less expensive than the noble gases their mixtures are being investigated. The properties of hydrogen-carbon dioxide mixtures are currently

being surveyed. The estimated variation in Prandtl number is plotted on Figure 10 for this mixture, it is seen that the minimum is Pr $\tilde{\sim}$ 0.34 at M $\tilde{\sim}$ 15. A supply at this molecular weight and at M $\tilde{\sim}$ 29 has been obtained for comparison to the data of section 2 and to extend our data to lower Pr.

On March 3, during a preliminary test with helium flow at a moderate heating rate the test section failed in the vicinity of the pressure tap attachment at x/D = 56. Inspection showed evidence of brittle fracture along grain boundaries as well as some molten regions. It is hypothesized that the tube failed due to intergranular fracture and that as the two sections parted the electric arc caused local melting. Failure analysis with scanning electron microscope and microprobe of the University's Space Sciences Center is planned. A new test section is under construction and should be installed by mid April.

5. CONVECTION HEAT TRANSFER FROM ROUGH SURFACES

Proposals for increasing the performance of current Brayton systems include operation at higher pressure levels, use of alternate fluids, increased use of roughness elements and extended surfaces, and selection of materials capable of higher temperatures. The highest temperatures are in the heating component. The proposed Gas Cooled Fast Breeder Reactor (GCFBR) and the defunct nuclear rocket propulsion program faced comparable requirements for high power densities. The GCFBR technology is planning on using helium at high pressure with artificially roughened coolant channels fabricated from high temperature alloys. On the other hand, the Nerva program chose graphite, pyrolitic carbon and niobium carbide to operate at higher temperatures than possible with metal alloys. Other proposals

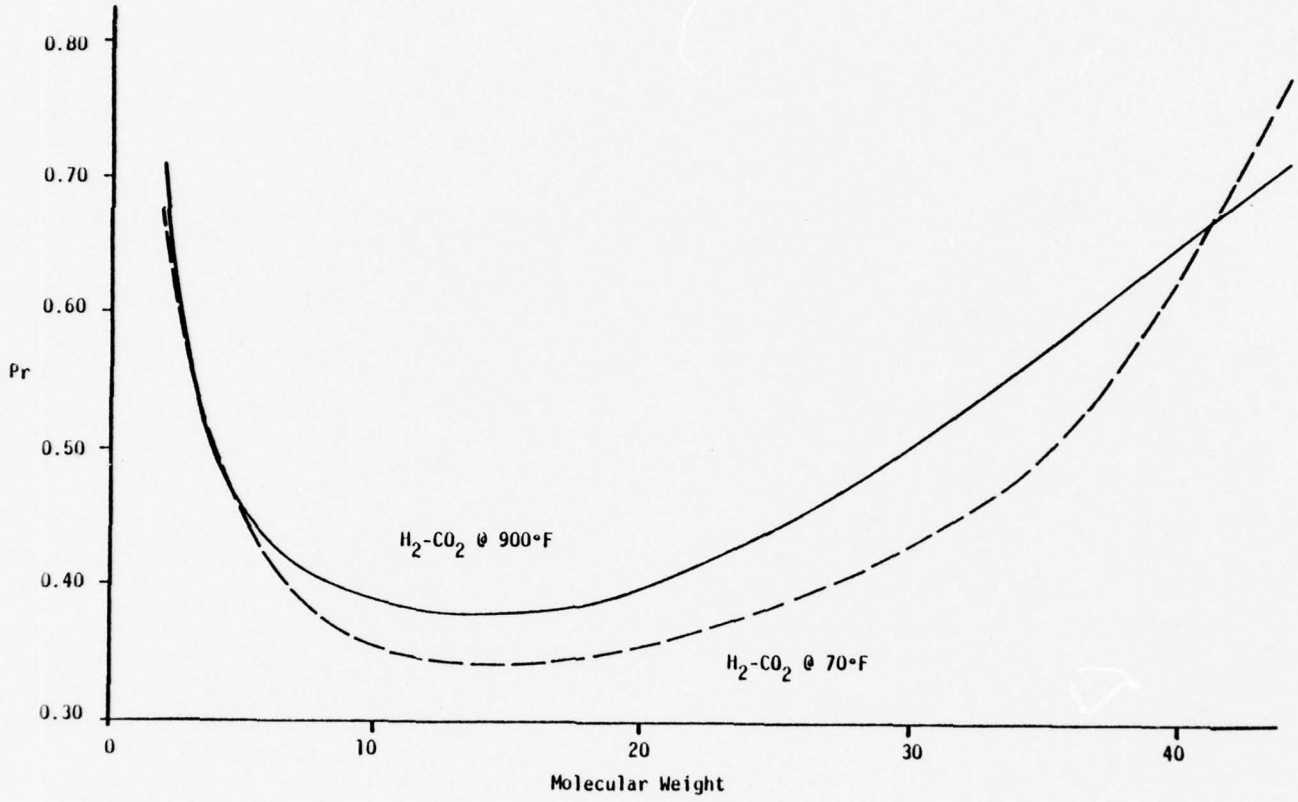

Figure 10. Estimated Properties of Hydrogen-Carbon Dioxide Mixtures

suggest using ceramics such as silicon nitride (Si_3N_4) for the heater and turbine blades. Each of these approaches potentially involves basic convection problems which have not been significant in existing small Brayton engines for Naval applications.

Our studies to date have concentrated on examining convective heat transfer and wall friction for alternate working fluids, the noble gases and their mixtures. The expense of the high molecular weight Noble gas mixtures leads to concern over the possibility of leakage in large scale plants. While such leakage is likely to be primarily the lower molecular weight- and cheaper-component, other mixtures of more common gases could be used to provide some of the advantages of the Noble gas mixtures at lower expense. Accordingly, we have begun measurements with alternate gas mixtures as described in the previous section.

Development of ceramic tubes for the heating component is critical to the success of the some proposed improved Brayton cycles. Likewise, ceramic turbine blades are suggested as a means of increasing turbine inlet temperatures without the need for internal blade cooling [Johansen and Wallace, 1976]. Fabrication studies show a rough surface with closely-spaced, approximately triangular, ribbed shape; the strength of blade depends strongly on the orientation of these ribs. With heating in an oxidizing atmosphere, the surface texture changes considerably in a few hours; one would expect a comparable variation during the operating life of an inert gas system at a low concentration of impurities such as residual air from initial changing of the system. The change in texture will modify the frictional pressure drop and convective heat transfer characteristics of the ceramic surface.

The estimated geometry of some typical roughened surfaces is presented in Table 4. Currently under design is a test section for measuring velocity and temperature distributions, heat transfer parameters and pressure drop for surfaces--representing both naturally occurring ceramic surfaces and artificially roughened superalloys--at heating rates causing significant property variations as for high power densities.

To increase power densities in the heater of a Brayton system for lightweight ship propulsion, the entire length of the coolant channel does not need to be roughened. For a thermal boundary condition of a specified heating rate, $q''_w(x)$, the tube wall temperature peaks in the downstream region of the channel. By using a rough surface only in the section with maximum wall temperatures, the peak value can be reduced below limits imposed by material limitations and/or the heating rate can be raised so the turbine inlet temperature is increased. The pressure drop is increased only in the vicinity of the rough surface so substantially larger heat transfer improvement can be accommodated locally without roughening the entire channel (and, thus, increasing the pressure drop throughout).

Basic data necessary for design include the development of the internal thermal and momentum boundary layers caused by the change in surface texture, the fully developed Stanton number and friction factor, and the redevelopment to a smooth wall boundary layer, all with heating rates causing significant property variation. Currently data are required for a variety of shapes, but advanced numerical methods for flows with recirculation may provide means to reduce experimentation in the future.

The experimental apparatus (Figure 11) is to use replaceable test sections so that various forms of roughness elements can be tested. The

Table 4. Characterization of Rough Surfaces (Typical Design Geometry - All Dimensions in Inches).

		h	w	P	D	h/D	P/h	
Typical artificially roughened alloy surface (rectangular ribs)	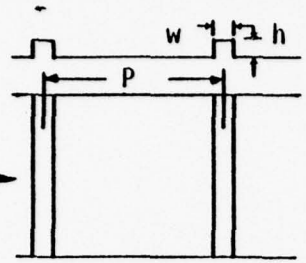	0.010	0.010	0.1	1	0.01	10	
Si_3N_4 Ceramic blade (as ground)	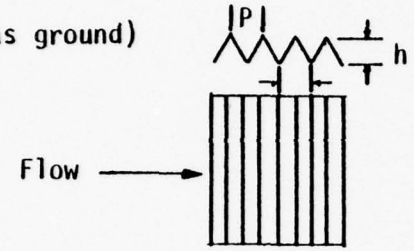	0.0002	0.0002	0.0002	0.5	0.0004	1	
Si_3N_4 Ceramic blade (oxidized) Random non-circular pits		0.0002 to 0.0008	0.0002 to 0.0008	0.0002 to 0.0008	0.5	0.0004 to 0.0016	1	
LWNPP(WADC) fuel elements	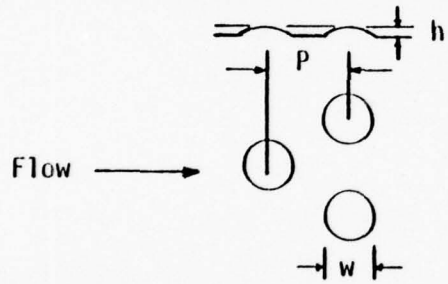	0.001 0.001	0.009 0.009	0.017 0.020	0.133 0.133	0.0075 0.0075	17 20	△ □

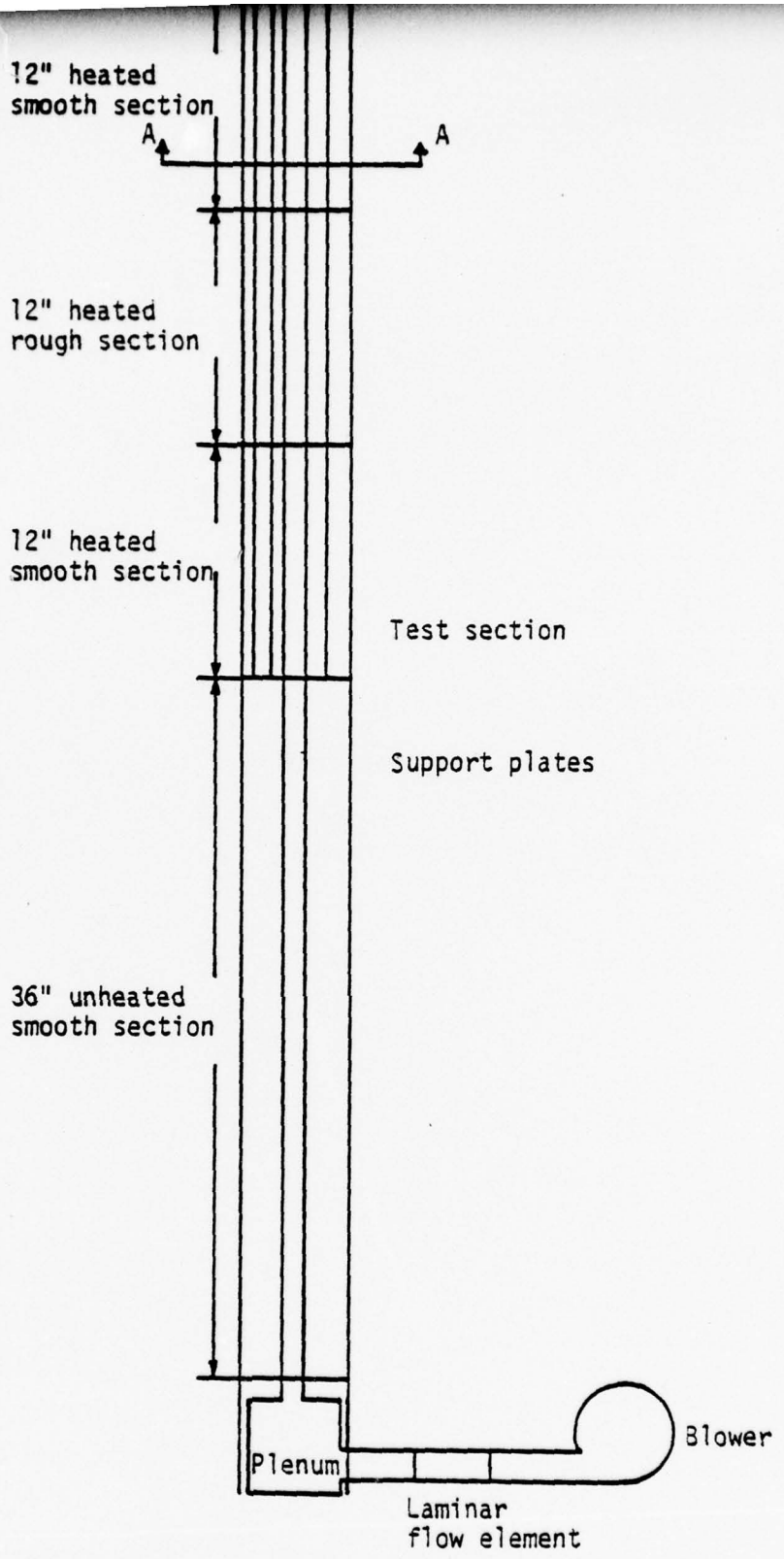

Figure 11. Apparatus for Measurements with Roughened Surfaces.

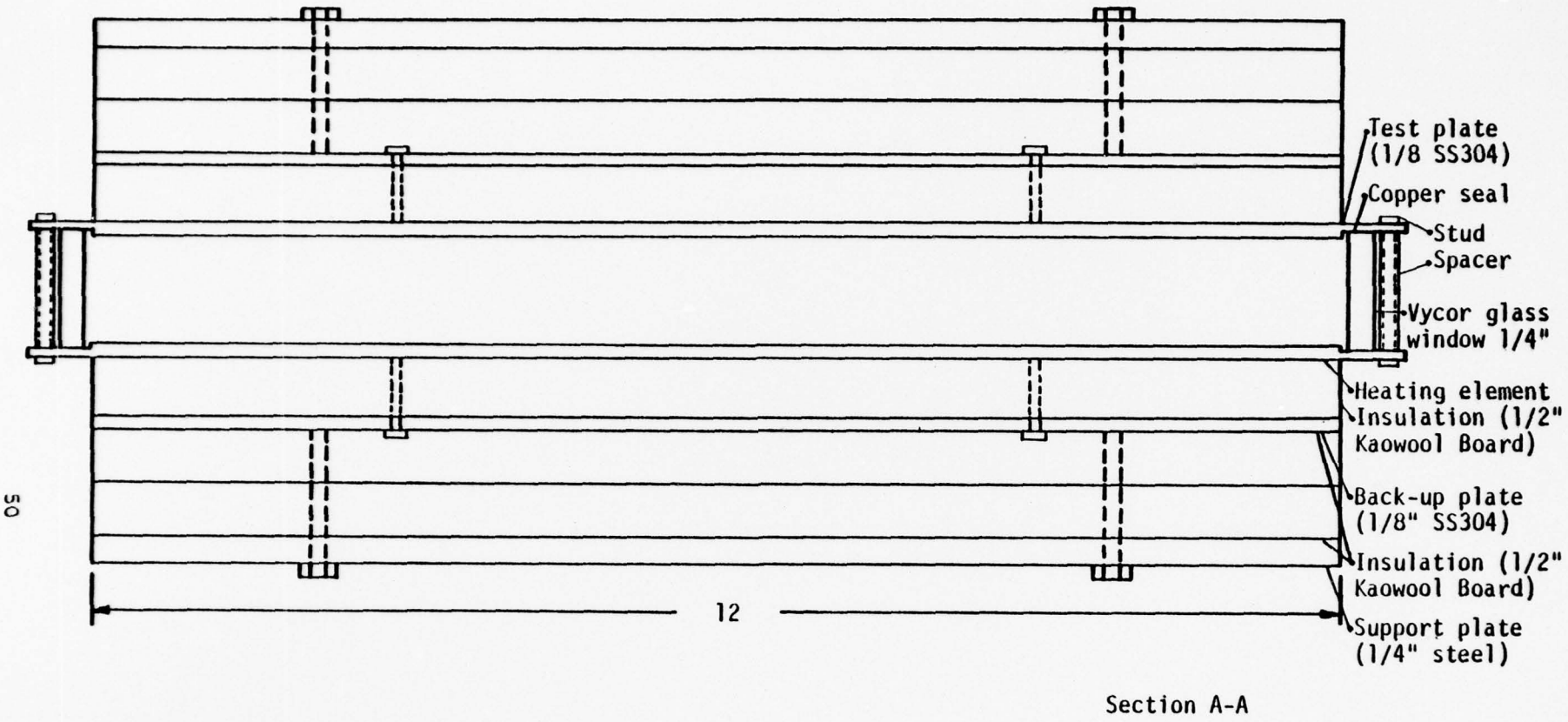

Figure 11.--continued

test section will consist of two electrically heated parallel plates about twelve inches wide, spaced one inch apart. Parallel plates are chosen to allow use of the laser Doppler anemometer for velocity measurement; one inch plate spacing is chosen to reduce natural convection effects in the initial measurements. A sketch of the initial heated plate is shown in Figure 12. Initial elements will be square ribs to extend existing data to examine the effect of heating rate through the temperature dependence of the properties. Pitch-to-height ratio, p/h, will be of the order of ten with h^+ about 20. A schematic diagram of the test section instrumentation has been shown earlier [McEligot, 1975a]. Air will be used as the gas ($Pr \tilde{\sim} 0.7$). Wall thermocouples and the power measurements provide the information to calculate local Stanton numbers. Temperature profile measurements will be made with a commercial hot wire anemometer operated as a resistance thermometer to determine thermal boundary layer development and the heat transfer roughness function,

$$G = t^+ - \frac{1}{\kappa Pr_t} \ell n(y/h)$$

The laser Doppler anemometer will be used to measure the axial velocity profile to deduce the momentum boundary layer development and the momentum transfer roughness function,

$$R = u^+ - \frac{1}{\kappa} \ell n(y/h)$$

The roughness functions provide the information necessary to set the boundary conditions to solve the energy equation and momentum equation numerically for design predictions.

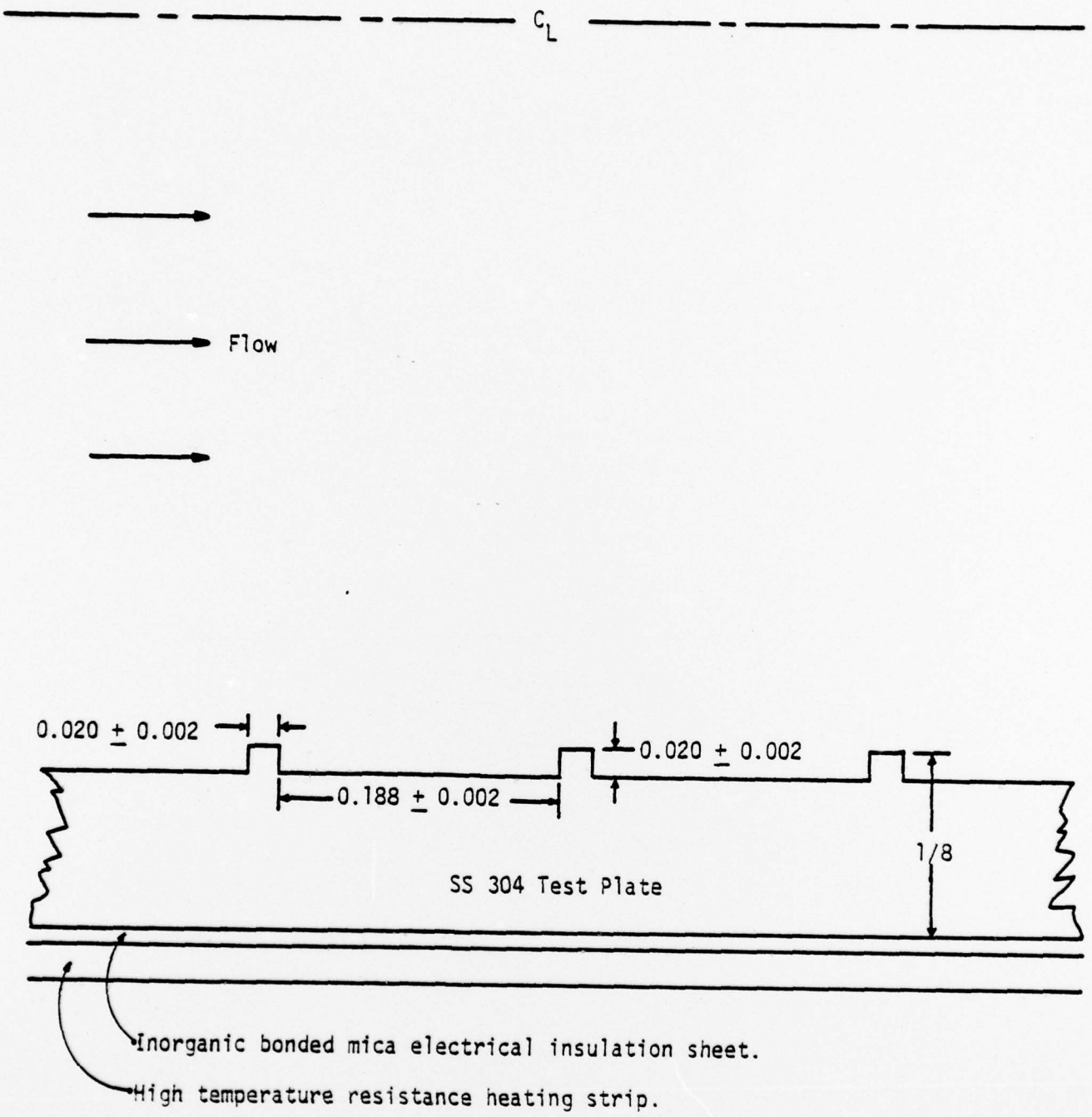

Figure 12. Initial Test Surface (to scale).

Currently, negotiations with fabricators are in progress for construction of the test surface and materials are on order. The single-component, laser Doppler anemometer system is complete with the exception of the TSI 1090 frequency tracker which is expected to be delivered in April. The receiving optics from OEI (Karlsruhe) were tested by the Principal Investigator at the Universität Karlsruhe during July 1976 prior to shipment.

6. CONCLUSIONS

The general goal of the project is to develop the ability to predict accurately temperature and velocity distributions, pressure drop and wall heat fluxes in components of the closed Brayton cycle. Since mixtures of inert gases offer advantages when used as the working fluid, the main emphasis of the present study has been to investigate the question whether existing design correlations for pure gas flows can be used reliably for such mixtures.

Examination of the properties of inert gas mixtures shows that, for concentrations providing improved heat transfer performance, the Prandtl number is reduced compared to pure gases. Heat transfer data have not previously been available in this range ($Pr < 0.5$) so the effect of the Prandtl number variation had not been measured. Since high power densities require high wall heat fluxes, large temperature differences may be encountered: calculations of mixture thermal conductivity and viscosity vary approximately as the 0.7 to 0.8 power of the absolute temperature.

Operating conditions for heat transfer components of Brayton cycle systems for Naval applications are expected to be:

Regenerative heat exchangers	plate/fin geometry, laminar or transitional flow, approximately constant wall heat flux
Heater	tubes or ducts, turbulent flow, specified wall heat flux distribution
Cooler	plate/fin geometry, laminar or transitional flow, approximately constant wall temperature

To simulate conditions in the heater, numerical analysis was applied to turbulent flow in a circular tube with constant wall heat flux. For constant fluid properties, it was predicted that the local Nusselt number would be reduced below the value given by the existing Dittus-Boelter correlation and Colburn analogy for gases; the reduction would become greater as the Prandtl number is decreased and Reynolds number is increased. These trends were confirmed by the experiments described below.

While numerical predictions for laminar flow require no empirical assumptions, turbulent flow predictions are based on the assumption of a turbulent Prandtl number. However, its dependence on molecular Prandtl number is not yet known so the turbulent predictions must be tested by experiment. Measurements of wall temperature and pressure drop were obtained in a vertical, resistively heated, circular tube with a nominal diameter of 1/8 inch (3mm) with a 92 diameter adiabatic entry followed by a 98 diameter heated section. Gases were air, helium and helium-argon mixtures of molecular weights approximately 15.8 and 29.7. The range of variables covered was Reynolds numbers from 30,000 to 102,000, Prandtl number from 0.42 to

0.7 and wall temperatures from room temperature to 1500°R, wall-to-bulk temperature ratios up to 1.9 and axial distances, $2.1 < x/D < 82$.

The data for heat transfer parameters were extrapolated to a wall-to-bulk temperature difference of zero to approximate the constant properties idealization. Comparison between these deduced data and numerical predictions based on hypothesized values of Pr_{tw}, the turbulent Prandtl number near the heated wall, provided estimates of the values of Pr_{tw}. Earlier tests had shown that for surface heating the resulting wall temperatures are primarily sensitive to Pr_{tw} and that values of Pr_t in the turbulent core are not particularly important. The turbulent Prandtl number in the wall region was deduced to be 1.1 ± 0.1 for $Pr \tilde{\sim} 0.42$, 1.0 ± 0.1 for $Pr \tilde{\sim} 0.49$ and 0.9 ± 0.1 for $Pr \tilde{\sim} 0.7$ for constant properties; variation with Reynolds number was slight. These results do not differ substantially from Reynolds analogy which is commonly employed in analyses.

With heating at conditions which caused property variation to be significant, the helium-argon data were correlated as

$$Nu = 0.021\ Re_b^{0.8}\ Pr_b^{0.55}\ [(T_w/T_b)^{-0.4} + 0.85\ D/x]$$

for $0.42 < Pr < 0.5$ to within ten percent for 92 percent of the data. The overall pressure drop data were correlated in terms of the average friction factor

$$f_{av} = (0.0014 + 0.125\ Re_w^{-0.32})(T_{w,av}/T_{b,av})^{-0.5}$$

The numerical analysis was extended to account for fluid property variation. For predictive purposes the value of Pr_{tw} was taken from the

results of the constant property study. Comparison to measurements with a helium-argon mixture of Pr = 0.49 showed the predictions to be adequate at $(T_w/T_b)_{max} \tilde{\sim} 1.8$ and $Re_i \tilde{\sim} 3 \times 10^4$.

To simulate conditions in the regenerative heat exchanger, numerical analysis was applied to laminar flow between parallel plates with constant wall heat flux. Our heat transfer results were reported earlier. For low temperature differences such that the fluid properties are approximately constant, the existing Sieder-Tate correlation was found to underpredict the Nusselt number substantially, to represent the Prandtl number dependence incorrectly and to vary with non-dimensional length L* in a different manner than the numerical predictions. A new correlation was obtained for the mean Nusselt number for simultaneous velocity and thermal boundary layer development,

$$Nu_a = [8.235^2 + 1.931^2/(Pr^{0.254}\ L^*)]^{1/2}$$

This correlation agrees with the predictions to within about five percent. In the entry region the mean Nusselt number increases about 17% as the Prandtl number is reduced to 0.2 from 2/3. It was found that when strong heating causes the fluid properties to vary significantly, the mean Nusselt number is only increased slightly above the value predicted by the constant property analysis provided the properties are evaluated at the average bulk temperature. If properties are evaluated at the average film temperature, the change in Nusselt number is greater and appears as a reduction rather than an increase.

For wall friction under the constant properties idealization, the average friction factor predicted by the numerical analysis can be approximated by

$$(f_a \cdot Re/24) = [1 + 0.0788/L^+]^{1/2}$$

to within ten percent for $L^+ \gtrsim 0.001$. In contrast to the heat transfer results, the bulk properties/property ratio method does not collapse the friction predictions well. However, in the range $-2 < Q^+ < 10$ the film temperature approach for evaluating fluid properties agrees with the constant properties friction relation above so it is recommended.

REFERENCES

Bammert, K.and R. Klein. (1974) "The Influence of He-Ne, He-N_2 and He-CO_2 Gas Mixtures on Closed Cycle Gas Turbines," ASME Paper 74-GT-124.

Bammert, K., J. Rurik and H. Griepentrog. (1974) "Highlights and Future Developments of Closed-cycle Gas Turbines," ASME Paper 74-GT-7.

Bankston, C. A., and D. M. McEligot. (1970) "Turbulent and Laminar Heat Transfer to Gases with Varying Properties in the Entry Region of Circular Ducts," Int. J. Heat Mass Transfer, 13, 319-344.

Blom, J. (1970) "Experimental Determination of the Turbulent Prandtl Number in a Developing Temperature Boundary Layer," Proc., Fourth Int. Heat Transfer Conf., Vol. 11, Paper FC 2.2.

Bodoia, J. R. and J. F. Osterle. (1961) "Finite Difference Analysis of Plane Poiseuille and Couette Flow Development," Appl. Sci. Research, 10A, 265-276.

Campbell, D. A. and H. C. Perkins. (1968) "Variable Property Turbulent Heat and Momentum Transfer for Air in a Vertical Rounded Corner Triangular Duct," Int. J. Heat Mass Transfer, 11, 1003-1012.

Cheung, H., L. A. Bromley and C. R. Wilke. (1962) "Thermal Conductivity of Gas Mixtures," A. I. Ch. E. Journal, 8, 221-228.

Dawe, R. A. and E. B. Smith. (1970) "Viscosities of the Inert Gases at High Temperature," J. Chem. Phys., 52, 693-703.

DiPippo, R. and J. Kestin. (1969) "The Viscosity of Seven Gases Up to 500°C and Its Statistical Interpretation," Fourth Symposium on Thermal Physical Properties, 304-313.

Drew, T. B., E. C. Koo and W. M. McAdams. (1932) "The Friction Factor in Clean, Round Pipes," Trans., Am. Inst. Chem. Engrs., 28, 56-72.

Gambhir, R. S. and S. C. Saxena. (1966) "Thermal Conductivity of Binary and Ternary Mixtures of Krypton, Argon and Helium," Mol. Phys., 11, 233-241.

Gandhi, J. M. and S. C. Saxena. (1968) "Correlated Thermal Conductivity Data of Rare Gases and Their Binary Mixtures at Ordinary Pressures," J. Chem. Engineering D., 13, 357-361.

Hess, W. G. (1965) "Thermocouple Conduction Error with Radiation Heat Loss," M.S.E. Thesis, University of Arizona.

Hilsenrath, J. C., W. Beckett, W. S. Benedict, L. Fano, H. J. Hoge, J. F. Masi, R. L. Nuttall, Y. S. Touloukian, and H. W. Wooley. (1955) Tables of Thermal Properties of Gases. NBS Circular 564.

Hirschfelder, J. O., C. F. Curtiss and R. B. Bird. (1964) Molecular Theory of Gases and Liquids, New York: Wiley.

Johansen, K. M. and R. E. Wallace. (1976) "Ceramic Gas Turbine Engine Demonstration Program," Interim Report No. 1, AiResearch Report No. 76-212188 (1), AiResearch Manufacturing Company.

Kalelkar, A. S. and J. Kestin. (1970) "Viscosity of He-Ar and He-Kr Binary Gaseous Mixtures in the Temperature Range 25-720°C," J. Chem. Phys., 52, 4248-61.

Kays, W. M. (1966) Convective Heat and Mass Transfer, New York: McGraw-Hill.

Kays, W. M. and A. L. London. (1964) Compact Heat Exchangers, 2nd Ed. New York: McGraw-Hill.

Kline, S. J. and F. A. McClintock. (1953) "The Description of Uncertainties in Single Sample Experiments," Mech. Engineering, 75, 38.

Kreith, F. (1958) Principles of Heat Transfer, Scranton: International Textbook Company.

Magee, P. M. and D. M. McEligot. (1968) "Effect of Property Variation on the Turbulent Flow of Gases in Tubes: The Thermal Entry," Nucl. Sci. Engineering, 31, 337-341.

Malina, J. A. and E. M. Sparrow. (1964) "Variable-property, Constant-property, and Entrance-region Heat Transfer Results for Turbulent Flow of Water and Oil in a Circular Tube," Chem. Eng. Sci., 19, 953-961.

Mason, E. A. and H. von Ubisch. (1960) "Thermal Conductivity of Rare Gas Mixtures," Phys. Fl., 3, 355-361.

Moen, W. K. (1960) "Surface Temperature Measurement," Inst. Control Syst., 33, 70-73.

Mock, E. A. (1970) "Closed Brayton Cycle System Optimization for Undersea, Terrestrial and Space Applications," von Karman Institute for Fluid Dynamics, Brussels, Belgium.

McAdams, W. H. (1954) Heat Transmission, 3rd Ed., New York: McGraw-Hill.

McEligot, D. M. (1974a,b,1975a,b) "Convection in the Closed Brayton Cycle," University of Arizona proposals 74-AME-28, 75-AME-42, 75-AME-95, 76-AME-35 submitted to ONR (Code 473).

McEligot, D. M., P. E. Pickett and M. F. Taylor. (1976) "Measurements of Wall Region Turbulent Prandtl Numbers in Small Tubes," Int. J. Heat Mass Transfer, 19, 799-803.

McEligot, D. M., M. F. Taylor and F. Durst. (1977) "Internal Forced Convection to Mixtures of Inert Gases," Int. J. Heat Mass Trans., 20, 475-486.

Peterson, J. N., T. F. Hahn and E. W. Comings. (1971) "Thermal Conductivity of Mixtures of Argon-Helium, Argon-Nitrogen and Argon-Neon," A. I. Ch. E. Journal, 17, 289-291.

Pickett, P. E. (1976) "Heat and Momentum Transfer to Internal, Turbulent Flow of Helium-Argon Mixtures in Circular Tubes," M.S.E. Report, Aerospace and Mechanical Engineering Department, University of Arizona.

Quarmby, A. and R. Quirk. (1972) "Measurements of the Radial and Tangential Eddy Diffusivities of Heat and Mass in Turbulent Flow in a Plain Tube," Int. J. Heat Mass Transfer, 15, 2309-2327.

Reichardt, H. (1951) "Complete Representation of Turbulent Velocity Distribution in Smooth Pipes," Z. Angew. Math. Mech., 31, 208.

Reynolds, A. J. (1975) "The Prediction of Turbulent Prandtl and Schmidt Numbers," Int. J. Heat Mass Transfer, 18, 1055-1069.

Reynolds, W. C. (1968) Thermodynamics, 2nd Ed., p. 228, New York: McGraw-Hill.

Reynolds, W. C. and H. C. Perkins. (1968) Engineering Thermodynamics, New York: McGraw-Hill.

Saxena, V. K. and S. C. Saxena. (1968) "Measurements of the Thermal Conductivity of Helium Using a Hot-Wire Type of Thermal Diffusion Column," Brit. J. Appl. Phys., (J. Phys. D.), I, 1341-1351.

Schade, K. W. and D. M. McEligot. (1971) "Cartesian Graetz Problems with Air Property Variation," Int. J. Heat Mass Transfer, 14, 653-666.

Schlünder, E. U. (1974) VDI-Wärmeatlas. Düsseldorf, VDI-Verlag.

Shah, R. K. and A. L. London. (1971) "Laminar Flow Forced Convection Heat Transfer and Flow Friction in Straight and Curved Ducts - A Summary of Analytical Solutions," Tech. Report 75, Mech. Eng., Stanford University.

Sleicher, C. A. and M. W. Rouse. (1975) "A Convenient Correlation for Heat Transfer to Constant and Variable Property Fluids in Turbulent Pipe Flow," Int. J. Heat Mass Transfer, 18, 677-683.

Taylor, M. F. (1967) "Correlation of Friction Coefficients for Laminar and Turbulent Flow with Ratios of Surface to Bulk Temperature from 0.35 to 7.35," NASA TR R-267.

Taylor, M. F., P. E. Pickett, F. Durst and D. M. McEligot. (1976) "Convection in the Closed Brayton Cycle," 2nd Annual Summary Report.

Touloukian, Y. S. and C. Y. Ho. (1970) Thermophysical Properties of Matter, Plenum Press, London.

Vanco, M. R. (1965) "Analytical Comparison of Relative Heat Transfer Coefficients and Pressure Drops of Inert Gases and Their Binary Mixtures," NASA TN-D-2677.

Van Driest, E. R. (1956) "On Turbulent Flow Near a Wall," J. Aeronaut. Sci., 23, 1007-1011 and 1036.

DISTRIBUTION LIST

Recipient	Number of Copies
Office of Naval Research 800 North Quincy Street Arlington, Virginia 22217 Attn: M. Keith Ellingsworth, Code 473	3
Defense Documentation Center Building 5 Cameron Station Alexandria, Virginia 22314	12
Naval Research Laboratory 4555 Overlook Avenue Washington, D. C. 20390 Attn: Technical Information Dvision	
Code 2627	6
Code 2629	6
Engineering Materials Division	1
U. S. Naval Postgraduate School Monterey, California 93940 Attn: Prof. P. F. Pucci, Mechanical Engineering	1
U. S. Naval Academy Annapolis, Maryland 21402 Attn: Department of Mechanical Engineering	1
Naval Sea Systems Command Crystal City, National Center #3 Washington, D. C. 20360 Attn: NSEA 033	1
NSEA 035	1
Naval Ships Engineering Center Century Building 4 Washington, D. C. 20362 Attn: NSEC 6147	1
NSEC 6146, Mr. J. W. Fairbanks	1
Naval Ships R & D Center Annapolis, Maryland 21402 Attn: Mr. Sid Cox	1

National Science Foundation
1800 G Street, N. W.
Washington, D. C. 20550 1

NASA Lewis Research Center
21000 Brookpark Road
Cleveland, Ohio 44135
Attn: Bert Probst 1

Defense Advanced Research Projects Agency
1400 Wilson Boulevard
Arlington, Virginia 22209
Attn: Dr. George Donahue 1

Maritime Administration
14th & E Streets. N. W.
Washington, D. C. 20230
Attn: Frank Critelli 1

Electric Power Research Institute
P. O. Box 10412
Palo Alto, California 94303
Attn: Dr. Arthur Cohn 1

Office of Naval Research
Resident Representative
University of Arizona
Room 421--Space Sciences Building
Tucson, Arizona 84721 1

Assistant Chief for Technology
Office of Naval Research, Code 200
Arlington, Virginia 22217 1

Dr. Rudolph J. Marcus
Office of Naval Research
Pasadena Branch Office
1030 East Green Street
Pasadena, California 91106 1

AiResearch Manufacturing Company of Arizona
402 S. 36th Street
P. O. Box 5217
Phoenix, Arizona 85010
Attn: Mr. Ray A. Rackley 2
Mr. Keith M. Johansen 1

AiResearch Manufacturing Company
2525 West 190th Street
Torrance, California 90509
Attn: Mr. Murray Coombs 1

Dr. W. H. Theilbahr
Naval Weapons Center (Code 3161)
China Lake, California 93555 1